J|A|C|S
ARTICLES
Published on Web 10/15/2002

Characteristic Reactions and Properties of *C*-Apical *O*-Equatorial (*O-cis*) Spirophosphoranes: Effect of the σ^*_{P-O} Orbital in the Equatorial Plane and Isolation of a Hexacoordinate Oxaphosphetane as an Intermediate of the Wittig Type Reaction of 10-P-5 Phosphoranes

Shiro Matsukawa,[†] Satoshi Kojima,[†] Kazumasa Kajiyama,[†] Yohsuke Yamamoto,[†] Kin-ya Akiba,*[,†,‡] Suyong Re,[§] and Shigeru Nagase[§]

Contribution from the Department of Chemistry, Graduate School of Science, Hiroshima University, 1-3-1 Kagamiyama, Higashi-Hiroshima 739-8526, Japan, the Advanced Research Center for Science and Engineering, Waseda University, 3-4-1 Ohkubo, Tokyo 169-8555, Japan, and the Department of Theoretical Studies, Institute for Molecular Science, Myodaiji, Okazaki 444-8585, Japan

Received May 3, 2002. Revised Manuscript Received August 16, 2002

Abstract: Novel spirophosphoranes (*O-cis*) that exhibit reversed apicophilicity having an apical carbon−equatorial oxygen array in a five-membered ring showed enhanced reactivity toward nucleophiles such as *n*-$Bu_4N^+F^-$ or MeLi in comparison with the corresponding stable isomeric spirophosphoranes (*O-trans*) having an apical oxygen−equatorial carbon configuration. The enhanced reactivity of the *O-cis* isomer could be explained by the presence of a lower-lying $\sigma^*_{P-O(equatorial)}$ orbital as the reacting orbital in the equatorial plane, whereas the corresponding orbital is a higher-lying $\sigma^*_{P-C(equatorial)}$ in the *O-trans* isomer. Density functional theory (DFT) calculation on the actual compounds provided theoretical support for this assumption. In addition, we found that the benzylic anion α to the phosphorus atom in *O-cis* benzyl phosphorane is much more stable than that generated from the corresponding *O-trans* compounds. The experimental results were considered to be due to the $n_C \rightarrow \sigma^*_{P-O}$ interaction in the *O-cis* anion, and this was confirmed by DFT calculations. Furthermore, the hexacoordinate anionic species derived from the reaction of the benzylic anion from *O-cis* benzylphosphorane with an aldehyde was also found to be stabilized as compared with analogous species from the corresponding *O-trans* isomer. The first X-ray structural characterization of a hexacoordinate phosphate intermediate in the Wittig type reaction using pentacoordinate phosphoranes is reported.

Introduction

Phosphoryl transfer, an important biological reaction involved in processes such as energy transfer and DNA formation, is generally assumed to involve pentavalent phosphorus intermediates (or transition states) formed by nucleophilic attack upon tetracoordinate phosphorus atoms, and it is assumed that the stability and stereochemistry (both steric and electronic effects combined) of the transient species (or transition state) greatly influence the outcome of the process.[1] Therefore, to deduce a basic understanding of the process,[2] much attention has been focused on the stereochemistry of the pentacoordinate state by using various model phosphoranes.[3] Through these studies, it was found that two characteristic aspects, apicophilicity[4] (a thermodynamic aspect) and pseudorotation[5] (a kinetic aspect), are important. As for apicophilicity, that is, the relative preference for substituents to occupy the apical positions as opposed to the equatorial positions in trigonal bipyramidal (TBP) structures, a number of experimental results[6] and theoretical calculations[7] have indicated that multiple factors are involved.

* Corresponding author. E-mail: akibaky@waseda.jp.
[†] Hiroshima University.
[‡] Waseda University.
[§] Institute for Molecular Science.

(1) (a) Hengge, A. C. *Acc. Chem. Res.* **2002**, *35*, 105−112 and references therein. (b) Sinott, M. *Comprehensive Biological Catalysis: A Mechanistic Reference*; Academic Press: San Diego, CA, 1998; Vol. 1, pp 517−542. (c) Engel, R. *Handbook of Organophosphorus Chemistry*; Marcel Dekker: New York, 1992. (d) Breslow, R.; Labelle, M. *J. Am. Chem. Soc.* **1986**, *108*, 2655−2659.
(2) (a) Westheimer, F. H. *Acc. Chem. Res.* **1968**, *1*, 70−78. (b) Thatcher, G. R. J.; Kluger, R. *Adv. Phys. Org. Chem.* **1989**, *25*, 99−265.
(3) (a) Uchimaru, T.; Stec, W. J.; Taira, K. *J. Org. Chem.* **1997**, *62*, 5793−5800. (b) Uchimaru, T.; Uebayashi, M.; Hirose, T.; Tsuzuki, S.; Yliniemela, A.; Tanabe, K.; Taira, K. *J. Org. Chem.* **1996**, *61*, 1599−1608. (c) Taira, K.; Uchimaru, T.; Storer, J. W.; Yliniemela, A.; Uebayashi, M.; Tanabe, K. *J. Org. Chem.* **1993**, *58*, 3009−3017. (d) Dejaegeve, A.; Lim, C.; Karplus, M. *J. Am. Chem. Soc.* **1991**, *113*, 4353−4355. (e) Pyle, A. M. *Science* **1993**, *261*, 709−714.
(4) (a) Akiba, K.-y. *Chemistry of Hypervalent Compounds*; Wiley-VCH: New York, 1999. (b) Holmes, R. R. *Pentacoordinated Phosphorus—Structure and Spectroscopy*; ACS Monograph 175, 176, Vol. I, II; American Chemical Society, Washington, DC, 1980. (c) Corbridge, D. E. C. *Phosphorus: An Outline of Its Chemistry, Biochemistry, and Technology*, 4th ed.; Elsevier: Amsterdam, 1990; Chapter 14, pp 1233−1256. (d) Burgada, R.; Setton, R. In *The Chemistry of Organophosphorus Compounds*; Hartley, F. R., Ed.; Wiley-Interscience: Chichester, Great Britain, 1994; Vol. 3, pp 185−272. (e) Martin, J. C. *Science* **1983**, *221*, 509−514. (f) Muetterties, E. L.; Mahler, W.; Schmutzler, R. *Inorg. Chem.* **1963**, *2*, 613−618.
(5) Berry, R. S. *J. Chem. Phys.* **1960**, *32*, 933−938.

10.1021/ja026776c CCC: $22.00

A general propensity deduced from these results is that electronegative substituents prefer the apical positions, while π donative or bulky ligands prefer the equatorial positions. As for pseudorotation, that is, the mutual positional exchange of a pair of apical ligands and a pair of equatorial ligands, the barrier is usually relatively low (calculated to be ca. 2−3 kcal/mol for PH_5), causing rapid pseudorotations in contrast to tetracoordinate phosphorus species that are ordinarily stereochemically rigid except in cases in which the substitution at phosphorus facilitates an edge-inversion process.[8,9]

One distinct difference between the more familiar chemistry of tetracoordinate carbon and that of pentacoordinate compounds such as phosphoranes is the number of possible stereoisomers. For simplicity, taking into account only asymmetry at the central atom, for the former carbon atom only a pair of enantiomers are possible, and thus in principle there is no difference in reactivity. On the other hand, for the latter phosphorus in trigonal bipyramidal structure, up to 10 pairs of diastereoisomers are possible, and thus a larger variety in reactivity is expected according to each pair. However, because of the presence of the pseudorotation process that allows stereoisomers to interconvert readily, it is not possible to distinguish the difference of reactivity among pseudorotamers. In a limited number of cases, there are reports on the observation of coexisting stereoisomers in which one apical and one equatorial substituent are exchanged.[10] However, in these cases, the barrier to pseudorotation is low, and thus these examples are not suitable for the examination of differences in reactivity. By utilizing the rigidity of the Martin bidentate ligand, we have successfully slowed pseudorotation enough to isolate enantiomeric pairs of optically active 10-P-5 phosphoranes[11] and to synthesize spirophosphoranes having an apical carbon−equatorial oxygen array in a five-membered ring (**1**: *O-cis*). The latter represents the first examples of 10-P-5 phosphorane pseudorotamers that violate the apicophilicity concept and can still be converted to their more stable pseudorotamers[12,13] of apical oxygen−equatorial carbon configuration (**2**: *O-trans*) (Scheme 1). This now provides the opportunity to investigate the difference in reactivity between isomeric phosphoranes differing only in stereochemistry upon the pentacoordinate phosphorus atom. Nucleophilic reactions at pentacoordinate compounds are generally considered to take place within the equatorial plane, with the nucleophile attacking one of the equatorial bonds from the rear side.[14] Thus, if this were true, **1** would be expected to be more reactive toward nucleophiles than its more stable counterpart **2**, since a lower-lying σ^*_{P-O} orbital is available in **1**, whereas the corresponding orbital is a higher-lying σ^*_{P-C} orbital in **2** (Scheme 2). We have found this to be experimentally true, and a theoretical investigation provided evidence for our rationale based upon orbital considerations. In addition, we have found that the benzylic anion α to the phosphorus atom in the *O-cis* form is much more stable than that derived from the corresponding *O-trans* benzyl phosphorane. Furthermore, the hexacoordinated anionic species derived from the reaction of an α-benzylic anion from *O-cis* benzyl phosphorane with an aldehyde was also found to be more stabilized as compared with the hexacoordinate species from the corresponding *O-trans* isomer. This has allowed us to carry out the first X-ray structural analysis of a hexacoordinated phosphate bearing an oxaphosphetane ring system, an intermediate in the Wittig type reaction involving pentacoordinated phosphoranes. Full details are given herein.

Scheme 1

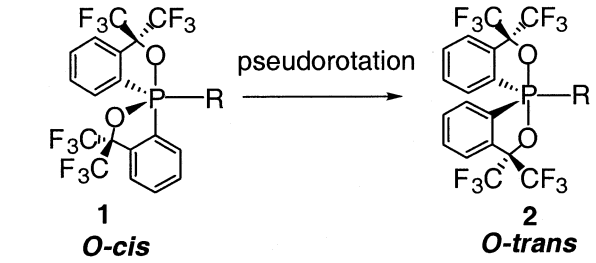

Scheme 2

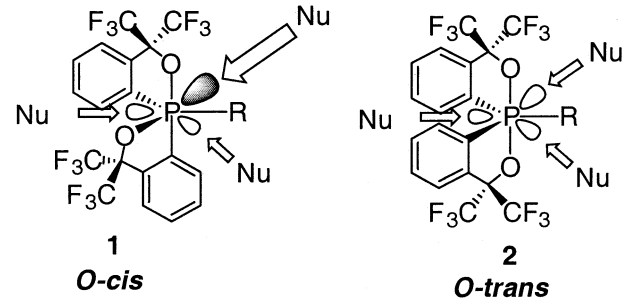

Results and Discussion

Preparation of *O-cis* Spirophosphoranes and Reactions with Nucleophiles. *O-cis* phosphoranes **1a** and **1b** (**1a**, R = Me; **1b**, R = *n*-Bu) were prepared by procedures recently

(6) (a) Nakamoto, M.; Kojima, S.; Matsukawa, S.; Yamamoto, Y.; Akiba, K.-y. *J. Organomet. Chem.* **2002**, *643*−*644*, 441−452. (b) Trippett, S. *Phosphorus Sulfur* **1976**, *1*, 89−98. (c) Trippett, S. *Pure Appl. Chem.* **1970**, *40*, 595−604. (d) Buono, G.; Llinas, J. R. *J. Am. Chem. Soc.* **1981**, *103*, 4532−4540. (e) Eisenhut, M.; Mitchell, H. L.; Traficante, D. D.; Kaufman, R. J.; Deutsch, J. M.; Whitesides, G. M. *J. Am. Chem. Soc.* **1974**, *96*, 5385−5397. (f) Moreland, C. G.; Doak, G. O.; Littlefield, L. B.; Walker, N. S.; Gilje, J. W.; Braun, R. W.; Cowley, A. H. *J. Am. Chem. Soc.* **1976**, *98*, 2161−2165. (g) Griend, L. V.; Cavell, R. G. *Inorg. Chem.* **1983**, *22*, 1817−1820.

(7) (a) Hoffmann, R.; Howell, J. M.; Muetterties, E. L. *J. Am. Chem. Soc.* **1972**, *94*, 3047−3058. (b) McDowell, R. S.; Streitwieser, A., Jr. *J. Am. Chem. Soc.* **1985**, *107*, 5849−5855. (c) Deiters, J. A.; Holmes, R. R.; Holmes, J. M. *J. Am. Chem. Soc.* **1988**, *110*, 7672−7681. (d) Wang, P.; Zhang, Y.; Glaser, R.; Reed, A. E.; Schleyer, P. v. R.; Streitwieser, A., Jr. *J. Am. Chem. Soc.* **1991**, *113*, 55−64. (e) Wasada, H.; Hirao, K. *J. Am. Chem. Soc.* **1992**, *114*, 16−27. (f) Thatcher, G. R. J.; Campbell, A. S. *J. Org. Chem.* **1993**, *58*, 2272−2281. (g) Wang, P.; Zhang, Y.; Glaser, R.; Streitwieser, A.; Schleyer, P. v. R. *J. Comput. Chem.* **1993**, *14*, 522−529. (h) Wladkowski, B. D.; Krauss, M.; Stevens, W. J. *J. Phys. Chem.* **1995**, *99*, 4490−4500.

(8) Moc, J.; Morokuma, K. *J. Am. Chem. Soc.* **1995**, *117*, 11790−11797 and references therein.

(9) (a) Dixon, D. A.; Arduengo, A. J., III; Fukunaga, T. *J. Am. Chem. Soc.* **1986**, *108*, 2461−2462. (b) Dixon, D. A.; Arduengo, A. J., III. *J. Phys. Chem.* **1987**, *91*, 3195−3200. (c) Dixon, D. A.; Arduengo, A. J., III. *J. Am. Chem. Soc.* **1987**, *109*, 338−341.

(10) (a) Lösking, O.; Willner, H.; Oberhammer, H.; Grobe, J.; Van, D. L. *Inorg. Chem.* **1992**, *31*, 3423−3427 and references therein. (b) Kawashima, T.; Soda, T.; Okazaki, R. *Angew. Chem., Int. Ed. Engl.* **1996**, *35*, 1096−1098.

(11) (a) Kojima, S.; Kajiyama, K.; Akiba, K.-y. *Tetrahedron Lett.* **1994**, *35*, 7037−7040. (b) Kojima, S.; Kajiyama, K.; Akiba, K.-y. *Bull. Chem. Soc. Jpn.* **1995**, *68*, 1785−1797.

(12) (a) Kojima, S.; Kajiyama, K.; Nakamoto, M.; Akiba, K.-y. *J. Am. Chem. Soc.* **1996**, *118*, 12866−12867. (b) Kajiyama, K.; Yoshimune, M.; Nakamoto, M.; Matsukawa, S.; Kojima, S.; Akiba, K.-y. *Org. Lett.* **2001**, *3*, 1873−1875.

(13) Some compounds violate the concept of apicophilicity. In these cases some sort of steric constraints disallowed regular configurations. (a) Timosheva, N. V.; Prakasha, T. K.; Chandrasekaran, A.; Day, R. O. (b) Timosheva, N. V.; Chandrasekaran, A.; Prakasha, T. K.; Day, R. O.; Holmes, R. R. *Inorg. Chem.* **1996**, *35*, 6552−6560. (c) Vollbrecht, S.; Vollbrecht, A.; Jeske, J.; Jones, P. G.; Schmutzler, R.; du Mont, W.-W. *Chem. Ber./Recl.* **1997**, *130*, 819−822.

(14) For example: Kojima, S.; Nakata, M.; Yamazaki, K.; Akiba, K.-y. *Tetrahedron Lett.* **1997**, *38*, 4107−4110.

Scheme 3

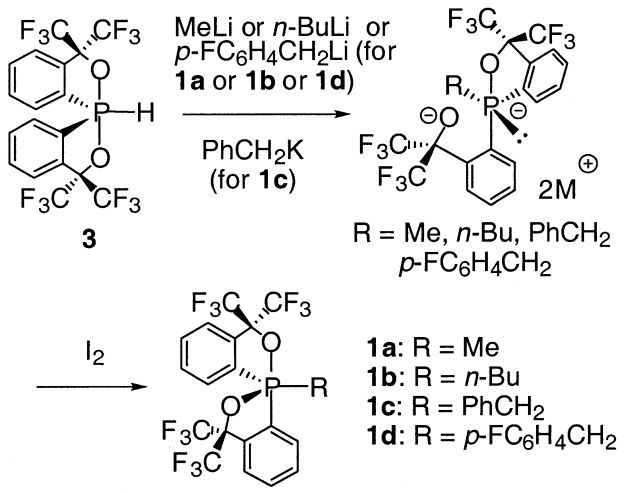

reported by us from the reaction of P−H phosphorane (**3**)[15] with 3 equiv of RLi, followed by treatment with I_2 (Scheme 3).[12b] *O-cis* benzyl phosphorane (**1c**) was prepared similarly from **3** with 3 equiv of benzylpotassium, which was generated by the reaction of "Superbase" with toluene. Similarly, a *p*-fluorophenylmethyl substituent could be introduced (**1d**). The structures of **1c** and **1d** were confirmed by X-ray analysis (Figure 1 (**1c**) and Supporting Information (**1d**)).

Reactions of *O-cis* **1b** and *O-trans* **2b** with nucleophiles were examined. Using TBAF (tetrabutylammonium fluoride; $(n\text{-Bu})_4N^+F^-$) as a nucleophile, the reaction of **1b** readily afforded a hexacoordinate phosphate (**4**) bearing a P−F bond (δ_P (THF): −105.0 ppm (d, $^1J_{P-F}$ = 706 Hz)) in THF at −30 °C, which was in equilibrium with **1b** (ratio of **4**/**1b** = 1:1) (Scheme 4). In contrast, **2b** did not react at all. The configuration of the phosphate **4** could not be determined with certainty because of rapid decomposition by trace amounts of H_2O. However, we have already characterized the corresponding hexacoordinate fluoroantimonate bearing two Martin ligands. The antimony analogue has the fluorine atom anti to one of the Martin ligand oxygens, which was shown by X-ray analysis. Although pseudorotation is a very low barrier process, especially in the presence of nucleophilic species for stiboranes, we determined the observed complex to be the thermodynamic product successfully, and the stabilization factor was attributed to the trans influence of the F−Sb−O bond.[16] Incidentally, this stable hexacoordinate species could be viewed as the immediate product of the attack of the fluoride anti to the Sb−O (equatorial) bond of the *O-cis* isomer, which in the case of antimony could not be observed because of facile pseudorotation. By analogy, in phosphate **4**, the fluorine atom is also likely to be located anti to an oxygen atom, and since equilibrium between **4** and **1b** can be observed, **4** should also be the thermodynamically most stable of all the plausible six isomeric hexacoordinate phosphates.

Similarly, *O-cis* **1b** reacted with 1 equiv of MeLi at 0 °C in 90 min to give the corresponding adduct **6b** (78% yield) after treatment with H_2O, while *O-trans* **2b**[17] was recovered unreacted under similar conditions (Scheme 5). Only under forcing conditions (5 equiv of MeLi at room temperature for 6 h) did **2b** slowly react with MeLi to give **6b** after hydrolysis (19%), along with a large amount of unreacted *O-trans* phosphorane **2b**. Since *O-cis* **1a** undergoes pseudorotation to give *O-trans* **2a** even at room temperature, the reaction of *O-cis* **1a** with MeLi was carried out at −23 °C for 3 h to diminish complications from competing pseudorotation. Phosphorane **6a** was obtained in 9.6% yield. Under the same conditions, *O-trans* **2a** was completely recovered intact. Hexacoordinate intermediates (**5a**, δ_P (THF) −104 ppm; **5b**, −83 and −92 ppm)[18] were observed in both reactions of **1a** and **b**. The adducts **6a** and **b** were

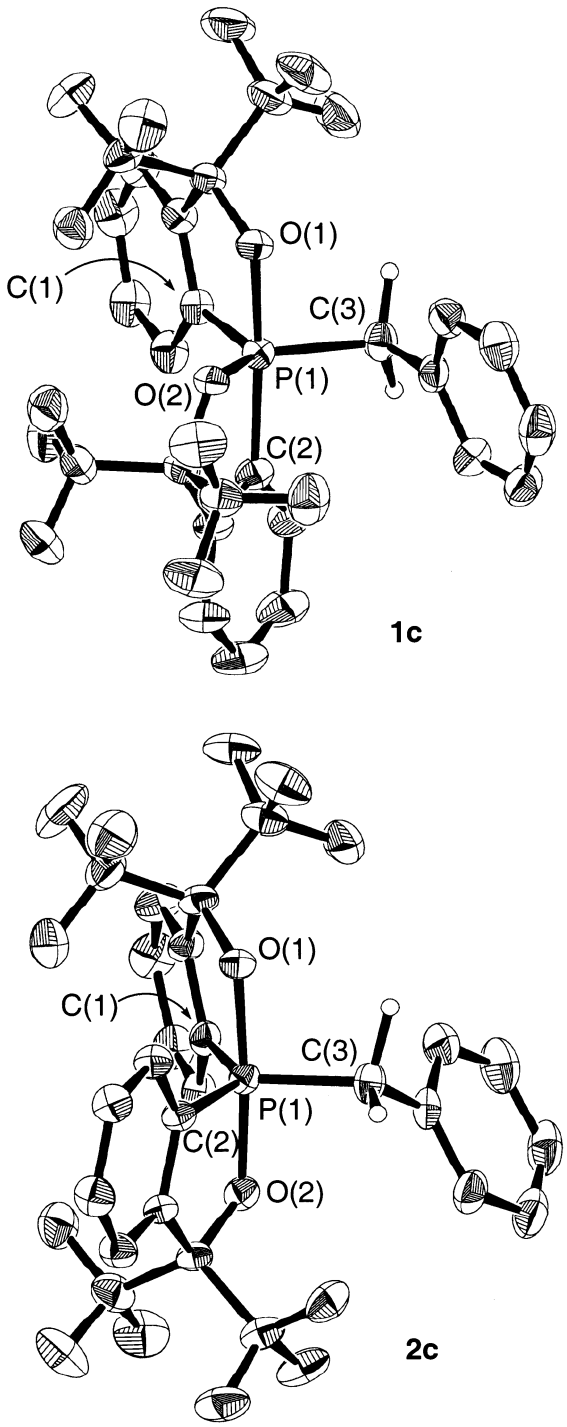

Figure 1. ORTEP drawings of **1c** and **2c** showing the thermal ellipsoids at the 30% probability level.

(15) Ross, M. R.; Martin, J. C. *J. Am. Chem. Soc.* **1981**, *103*, 1234−1235.
(16) Kojima, S.; Doi, Y.; Okuda, M.; Akiba, K.-y. *Organometallics* **1995**, *14*, 1928−1937.
(17) Kajiyama, K.; Kojima, S.; Akiba, K.-y. *Tetrahedron Lett.* **1996**, *37*, 8409−8412.

Scheme 4

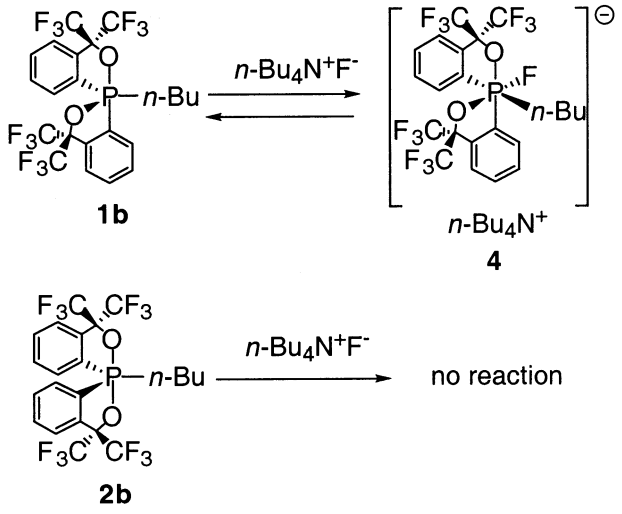

Scheme 5

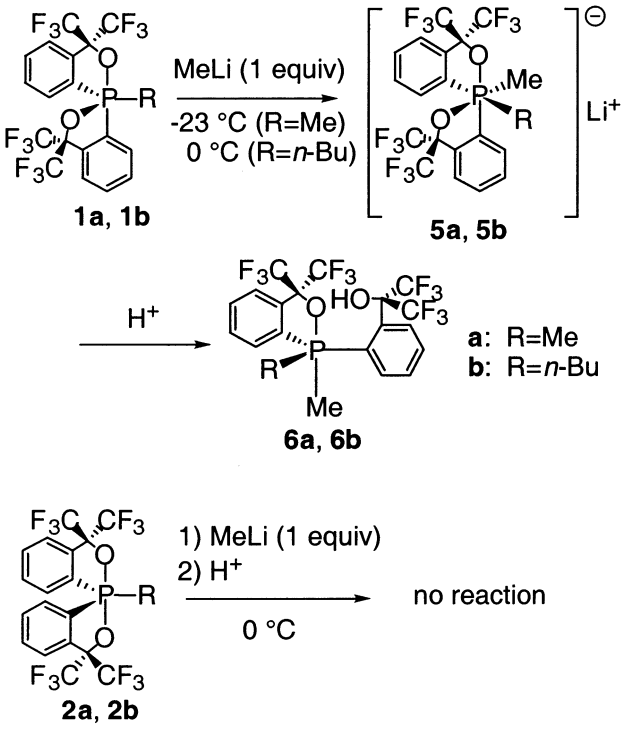

characterized by spectroscopic data, elemental analysis, and X-ray analysis (see Supporting Information).

Stabilization of Lone Pair Electrons Adjacent to the Phosphorus Atom of *O-cis* 1: Effect of σ^*_{P-O} Orbital in the Equatorial Plane on Stabilizing the α-Anion. Because the yield of **6a** could not be improved even after prolonged reaction (6 h) of **1a** with MeLi at 0 °C, we realized that this was due to the occurrence of facile deprotonation at the methyl group α to the phosphorus atom instead of nucleophilic attack. Thus, we decided to compare the behavior of *O-cis* and *O-trans* phosphoranes toward base by examining products resulting from the treatment with D_2O instead of H_2O after the addition of base. Because of complications arising from the fast pseudorotation from *O-cis* **1a**, we decided to look into the behavior of *O-cis* **1c** and *O-trans* **2c**[19] toward several bases in THF. Using

(18) The reason two signals were observed is unclear at present.

Scheme 6

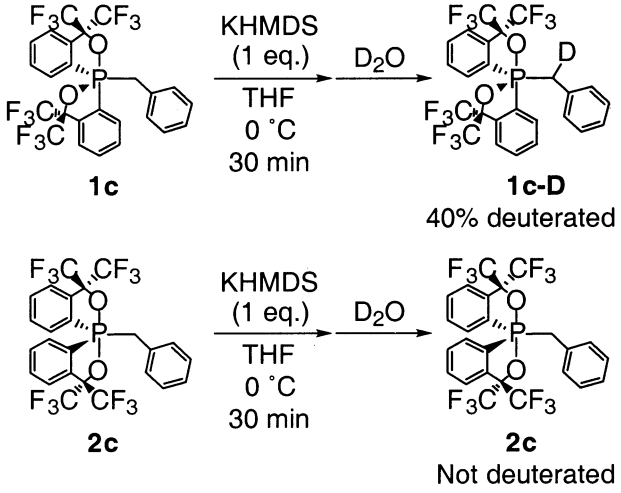

equimolar *n*-BuLi as base, *O-cis* **1c** was completely deprotonated within 5 min, and similarly, *O-trans* **2c** could also be converted to the corresponding anion. KH was also effective for **1c**, and deprotonation was achieved within 15 min at room temperature. However, deprotonation from **2c** using only KH was quite slow and was not complete even after 6 h. In this case, complete deprotonation required the use of 18-crown-6 ether as an additive. A clear difference was observed between **1c** and **2c** in the reaction with KHMDS (potassium hexamethyldisilazide; $(Me_3Si)_2N^-K^+$). Deprotonation of **1c** with KHMDS occurred in THF at 0 °C in 30 min and gave α-deuterated product (40% yield) after quenching the mixture with D_2O. On the other hand, **2c** could not be deprotonated under the same conditions (Scheme 6). These results indicated that the benzyl protons of *O-cis* **1c** were more acidic than those of *O-trans* **2c**. However, since there was the possibility that the distinct difference in reactivity was of a kinetic nature, an equilibration reaction between preformed *O-trans* anion **8c** and neutral *O-cis* **1c** was carried out. When *O-cis* **1c** was added to a solution of *O-trans* anion **8c-K(18-crown-6)**, equilibration took place rapidly, and the equilibrium completely shifted toward *O-cis* anion **7c-K(18-crown-6)** and neutral *O-trans* **2c** (Scheme 7). Thus, the higher acidity of the *O-cis* **1c** in comparison with *O-trans* **2c** was confirmed to be of a thermodynamic nature. The increased acidity of *O-cis* **1c** in comparison with *O-trans* **2c** would be due to the $n_C \rightarrow \sigma^*_{P-O}$ interaction in *O-cis* anion **7c**, which is expected to be much larger than the $n_C \rightarrow \sigma^*_{P-C}$ interaction in *O-trans* anion **8c-M** (Figure 2). The higher acidity of α-protons of the *O-cis* series as compared with those of the *O-trans* counterparts was supported by density functional theory (DFT) calculations (vide infra) on **1a**.

Before resorting to theoretical calculations, the spectral properties of the anions were briefly examined by means of ^{31}P NMR to determine whether the structural factors might assist in stabilizing the *O-cis* structures. In the case of *O-trans* phosphoranes, chemical resonances shifted to higher-field when **2c** (δ −21 ppm) was converted to **8c-M** (M = Li, K; δ −34 ppm), regardless of which metal was the countercation. In contrast, apart from the ^{31}P NMR chemical shift of the parent **1c** (δ −7 ppm), the lithium salt of *O-cis* **7c-Li** showed a

(19) Kojima, S.; Kawaguchi, K.; Akiba, K.-y. *Tetrahedron Lett.* **1997**, *38*, 7753−7756. A full account that includes the kinetic data of olefin formation is currently in preparation.

Scheme 7

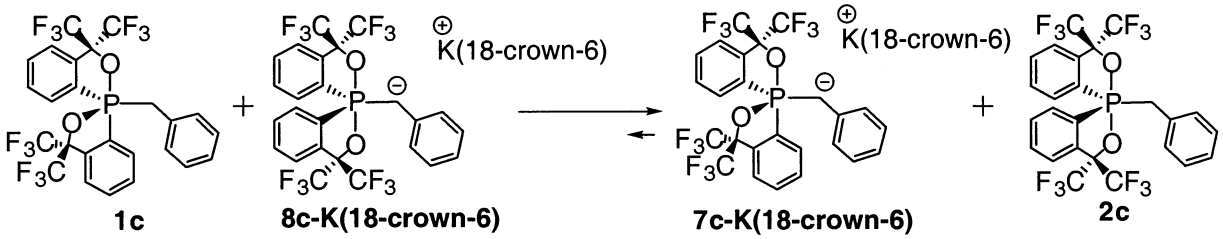

significantly different chemical shift (δ 2 ppm) from those of potassium (**7c-K**: δ −15 ppm), potassium 18-crown-6 (**7c-K-(18-crown-6)**: δ −25, −32 ppm (ratio 6:4)), or potassium [2.2.2]cryptand (**7c-K(cryptand)**: δ −25, −32 ppm (ratio 2:1)) salt. Therefore, **7c-Li** may be stabilized by coordination of the lithium cation with the two cis oxygen atoms in the *O-cis* framework. However, in the cases of **7c-K(18-crown-6)** and **7c-K(cryptand)**, such chelation effects would be expected to be small based on the similar chemical shifts, although an aggregation effect may be operative even in these cases because the compounds showed two different ^{31}P NMR signals. It is also possible that the two signals correspond to rotational isomers around the P−C(benzyl) bond having a double bond character (vide infra), since they were observed only for **7c**, not for **8c**.

In ^{13}C NMR, coupling constants ($^1J_{P-C}$) of the anions (220 Hz in **7c-K** and 227 and 228 Hz in **7c-K(18-crown-6)**, 215 Hz in **8c-K(18-crown-6)**) were almost twice as much as those of the corresponding neutral phosphoranes (107 Hz in **1c** and 112 Hz in **2c**). These results indicate the contribution of double bond character between the central phosphorus atom and the anionic benzyl carbon (Figure 2). This increase in coupling constants is similar to that observed for the change from phosphonium salt to the corresponding phosphorus ylide, which is generally considered to be of high double bond character.[20]

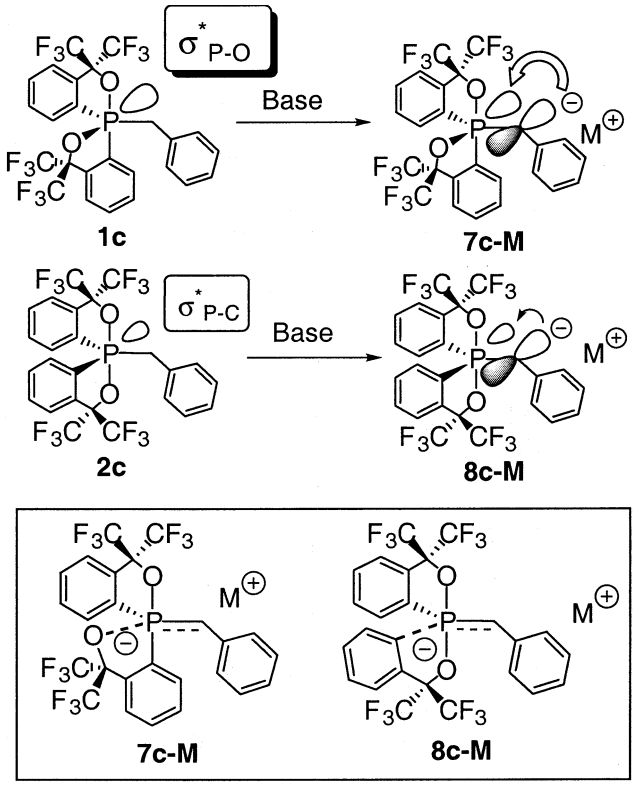

Figure 2. Effect of σ^*_{P-O} orbital in the equatorial plane in **1** on stabilizing the α-carbanion.

Theoretical Study on *σ Orbitals of *O-cis* and *O-trans* Phosphoranes in the Equatorial Plane and on the Stability of α-Anions from *O-cis* and *O-trans* Phosphoranes.** The structures of *O-cis* (**1a**) and *O-trans* (**2a**) phosphoranes with a methyl group as a monodentate ligand were optimized with DFT at the hybrid B3PW91 level,[21] using the Gaussian 98 program.[22] The basis sets employed were 6-31G(d)[23] for C, N, O, and H and 6-311G(2d)[24] for P. The calculated bond distances around the phosphorus atom are shown in Table 1, and they agree with the experimental values of **1b**−**d**[12a] and **2a**−**c**[12a] (for experimental details of **2a** and **c**, see Supporting Information), although the calculated P−O and P−C distances of **1a** and **2a** are slightly longer than the experimental values. Since the σ^*_{P-X} orbitals in the equatorial plane are responsible for nucleophilicity, we looked for such orbitals. These were found as a LUMO+4 for **1a** and as a LUMO+5 for **2a**, as shown clearly in Figure 3. Other LUMOs lying lower in energy below σ^*_{P-X} (X = O or C) were distributed on the aromatic rings of the Martin ligands as π^* orbitals. It should be noted that the σ^*_{P-O} level of **1a** (LUMO+4) is 18.7 kcal/mol lower than the σ^*_{P-C} level of **2a** (LUMO+5). Apparently, this large energy difference between σ^*_{P-O} and σ^*_{P-C} orbitals leads to a great enhancement of the reactivity of *O-cis* spirophosphorane **1** as compared with *O-trans* isomer **2**, as shown in Scheme 2.

Calculations were also carried out for *O-cis* anion (**7a**) and the corresponding *O-trans* anion (**8a**). The optimized structures are shown in Figure 4. Table 2 compares the equatorial distances in *O-cis* **1a**, *O-trans* **2a**, and their corresponding anions **7a** and **8a**. For both **7a** and **8a**, the three atoms constituting the CH_2 group make a coplanar (sp^2) plane, which is almost perpendicular to the equatorial plane. This implies that the lone pair on the carbon atom in the equatorial plane can be involved in a $n_C \rightarrow \sigma^*_{P-X}$ (equatorial) interaction (Figure 2). Accordingly, both anions (**7a** and **8a**) are stabilized by the $n_C \rightarrow \sigma^*_{P-X}$

(20) Kalinowski, H.-O.; Berger, S.; Braun, S. *Carbon 13 NMR Spectroscopy*; Wiley: Chichester, Great Britain, 1988; Chapter 4, pp 586−594.
(21) (a) Becke, A. D. *Phys. Rev.* **1988**, *A38*, 3098−3100. (b) Becke, A. D. *J. Chem. Phys.* **1993**, *98*, 5648−5652. (c) Perdew, J. P.; Wang, Y. *Phys. Rev.* **1992**, *B45*, 13244−13249.
(22) Frisch, M. J.; Trucks, G. W.; Schlegel, H. B.; Scuseria, G. E.; Robb, M. A.; Cheeseman, J. R.; Zakrzewski, V. G.; Montgomery, J. A., Jr.; Stratmann, R. E.; Burant, J. C.; Dapprich, S.; Millam, J. M.; Daniels, A. D.; Kudin, K. N.; Strain, M. C.; Farkas, O.; Tomasi, J.; Barone, V.; Cossi, M.; Cammi, R.; Mennucci, B.; Pomelli, C.; Adamo, C.; Clifford, S.; Ochterski, J.; Petersson, G. A.; Ayala, P. Y.; Cui, Q.; Morokuma, K.; Malick, D. K.; Rabuck, A. D.; Raghavachari, K.; Foresman, J. B.; Cioslowski, J.; Ortiz, J. V.; Stefanov, B. B.; Liu, G.; Liashenko, A.; Piskorz, P.; Komaromi, I.; Gomperts, R.; Martin, R. L.; Fox, D. J.; Keith, T.; Al-Laham, M. A.; Peng, C. Y.; Nanayakkara, A.; Gonzalez, C.; Challacombe, M.; Gill, P. M. W.; Johnson, B. G.; Chen, W.; Wong, M. W.; Andres, J. L.; Head-Gordon, M.; Replogle, E. S.; Pople, J. A. *Gaussian 98*, revision A.5; Gaussian, Inc.: Pittsburgh, PA, 1998.
(23) Francl, M. M.; Pietro, W. J.; Hehre, W. J.; Binkley, J. S.; Gordon, M. S.; DeFrees, D. J.; Pople, J. A. *J. Chem. Phys.* **1982**, *77*, 3654−3665.
(24) McLean, A. D.; Chandler, G. S. *J. Chem. Phys.* **1980**, *72*, 5639−5648.

Table 1. Selected Bond Distances (Å) for **1a**, **1b**,[12a] **1c**, **1d**, **2a**, **2b**,[12a] and **2c**

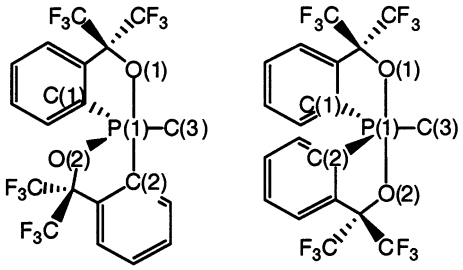

1 (*O-cis*) **2** (*O-trans*)

	Calculated		Experimental					
	1a	**2a**	**1b**[a]	**1c**	**1d**	**2a**	**2b**[a]	**2c**
P(1)−O(1)	1.769	1.769	1.773(3)	1.782(2)	1.766(3)	1.762(2)	1.765(2)	1.765(3)
P(1)−O(2)	1.665	1.764	1.658(2)	1.661(2)	1.667(2)	1.757(2)	1.750(2)	1.766(3)
P(1)−C(1)	1.828	1.822	1.806(4)	1.812(3)	1.808(3)	1.825(2)	1.822(2)	1.824(3)
P(1)−C(2)	1.876	1.822	1.860(4)	1.874(3)	1.876(4)	1.819(2)	1.817(2)	1.817(4)
P(1)−C(3)	1.827	1.818	1.830(5)	1.849(3)	1.849(4)	1.814(2)	1.818(3)	1.845(4)

[a] These values are revised ones furnished by resolving the structures.

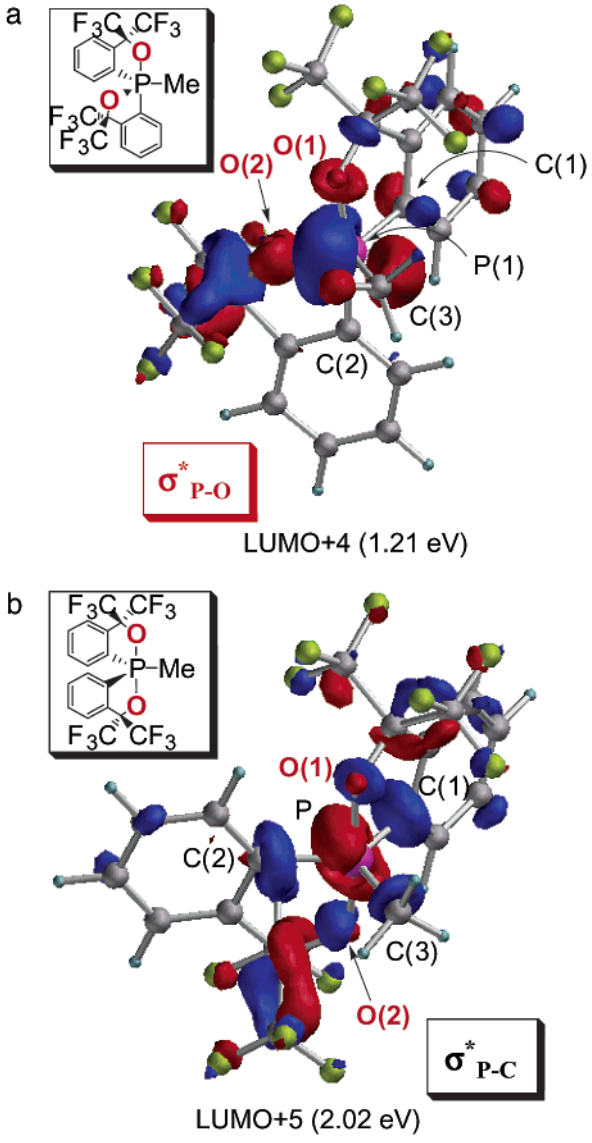

Figure 3. Calculated molecular orbitals and the energies of σ^*_{P-O} orbital in **1** and σ^*_{P-C} orbital in **2**, which should be responsible for the difference in the nucleophilic attack.

Table 2. Comparison of Calculated Bond Distances (Å) between Neutral (**1a** and **2a**) and Anionic Phosphoranes (**7a** and **8a**)

O-cis		**1a**	**7a**	increment
equatorial	P(1)−C(1)	1.828	1.854	+0.026 (+1.4%)
	P(1)−O(2)	1.665	1.758	**+0.093 (+5.6%)**
	P(1)−C(3)	1.827	1.667	**−0.160 (−8.8%)**
apical	P(1)−O(1)	1.769	1.839	+0.070 (+4.0%)
	P(1)−C(2)	1.876	1.887	+0.011 (+0.6%)
O-trans		**2a**	**8a**	increment
equatorial	P(1)−C(1)	1.822	1.857	+0.035 (+1.9%)
	P(1)−C(2)	1.822	1.856	+0.034 (+1.9%)
	P(1)−C(3)	1.818	1.668	**−0.150 (−8.3%)**
apical	P(1)−O(1)	1.769	1.823	+0.054 (+3.1%)
	P(1)−O(2)	1.764	1.823	+0.059 (+3.3%)

interaction, and this is reflected in the P−C(3) bond distances that are much shorter than the corresponding distances in **1a** and **2a**. The double bond character is consistent with the large P−C coupling constants in the anions. Although the degrees of P−C(3) bond shortening are similar in **7a** and **8a**, the degrees of elongation in the other equatorial bonds are quite different. Notably, the equatorial P−O bond is ca. 0.1 Å longer in **7a** than in **1a**, whereas the P−C bond in the *O-trans* anion is only 0.04 Å longer than that in **2a**. This suggests that the interaction is considerably stronger in **7a** than in **8a**, and thereby the anion is more stabilized in **7a** because of the larger electron delocalization. The stability of **7a** and **8a** is reflected in the relative energies. While the energy difference between **1a** and **2a** is as large as 14.1 kcal/mol, it is reduced to only 4.7 kcal/mol between **7a** and **8a** (Figure 3). The difference of 9.4 kcal/mol corresponds to an increase in the acidity of *O-cis* phosphorane **1a** as compared with *O-trans* phosphorane **2a**, at least in the gas phase. This is consistent with the observation that the acidity of the benzyl protons in *O-cis* **1c** is more enhanced than that of *O-trans* **2c**, as shown in Scheme 7.

Reaction of the α-Anion from *O-cis* 1c: Stabilization of Hexacoordinated Anions Derived from the Reaction of the α-Anion from *O-cis* 1c (Trans Influence of the P−O Bond). (i) Bromination and Acylation. With the anions in hand, several reactions of the anions were carried out, and we found

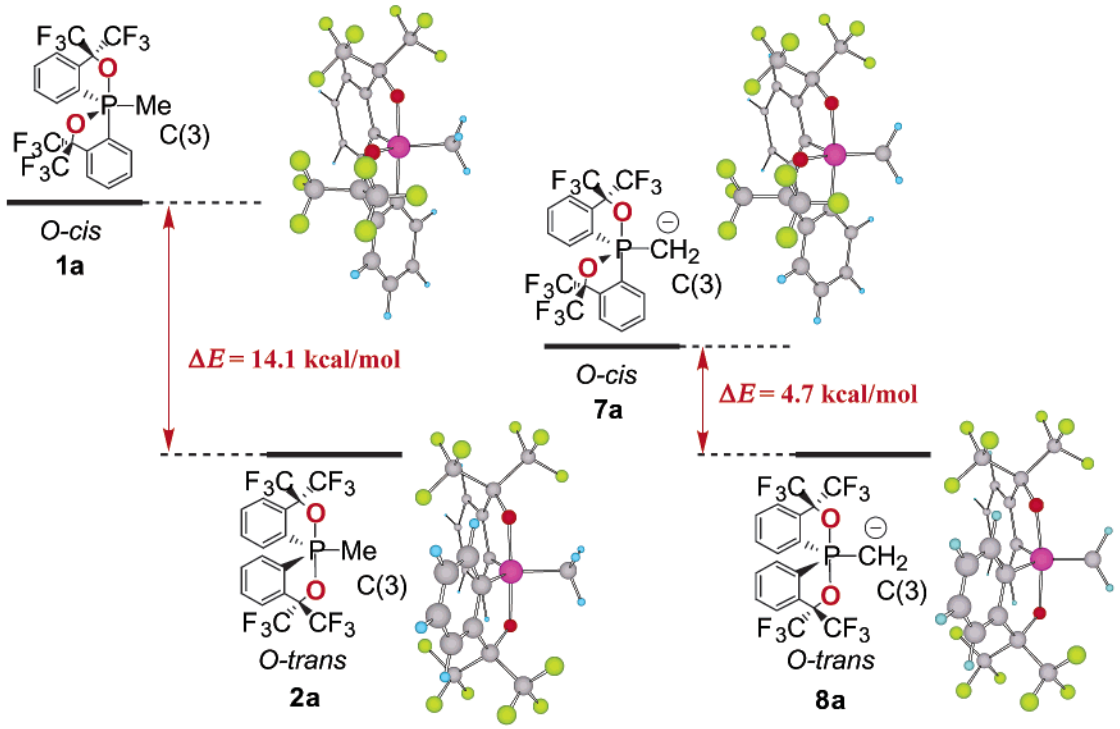

Figure 4. Calculated structures and the energies of **1a** and **2a** and the conjugated bases (**7a** and **8a**).

Scheme 8

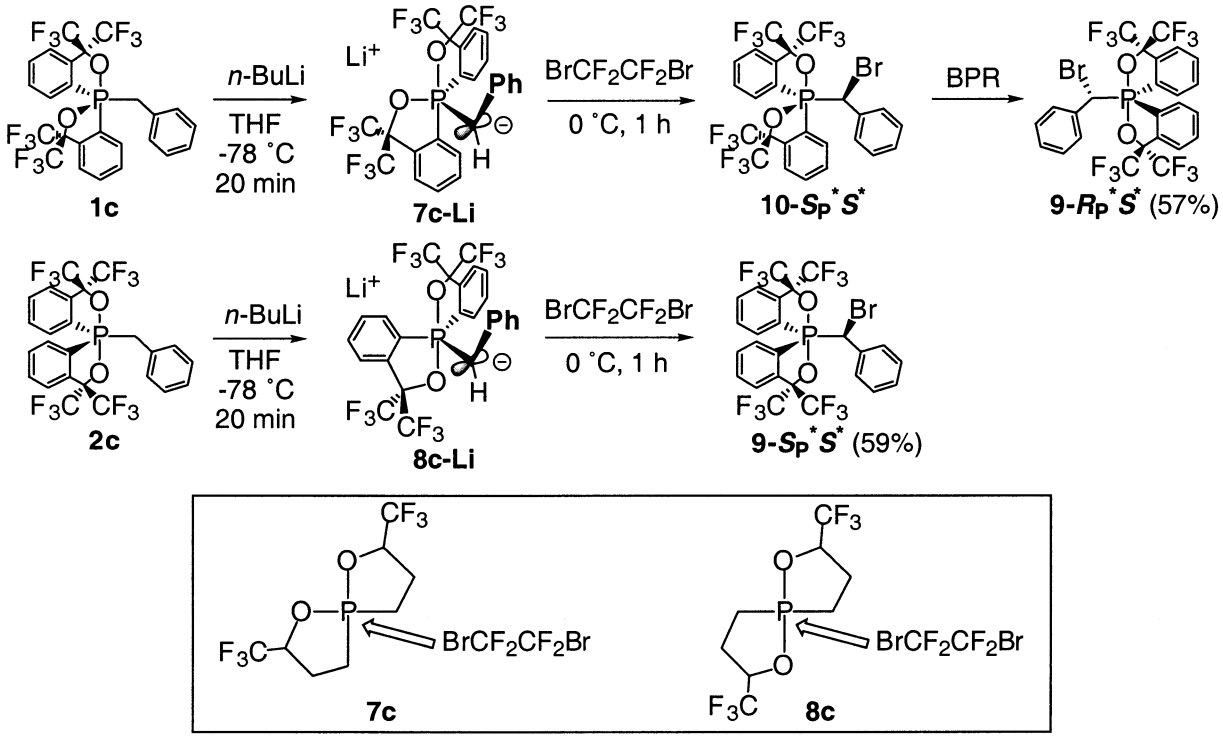

notable differences in the stability of the reaction products and the stereochemical results of the reactions. For example, bromination of the anion from *O-trans* **2c** by $BrCF_2CF_2Br$ afforded **9-*S*$_P$**S***** as the major product in an ca. 12:1 ratio as a result of direct bromination of the anion, whereas that from *O-cis* **1c** furnished **9-*R*$_P$**S***** as the predominant product in an ca. 12:1 ratio as a result of bromination followed by pseudorotation (Scheme 8). Recrystallization from *n*-hexane provided pure products for both cases. The relative configurations of **9-*R*$_P$**S***** and **9-*S*$_P$**S***** were determined by X-ray analysis (see Supporting Information). In the case of the reaction from *O-cis* **1c**, the electronegative nature of the bromine substituent at the α-position in *O-cis* phosphorane **10** is probably the reason for the acceleration of pseudorotation to the corresponding *O-trans* isomer **9-*R*$_P$**S*****. In the case of the reaction of *O-trans* **2c**, the major product **9-*S*$_P$**S***** does not undergo pseudorotation to its enantiomeric *O-trans* **9-*R*$_P$**S***** at ambient temperatures. Therefore, the observed product ratio reflects the selectivity in the

Scheme 9

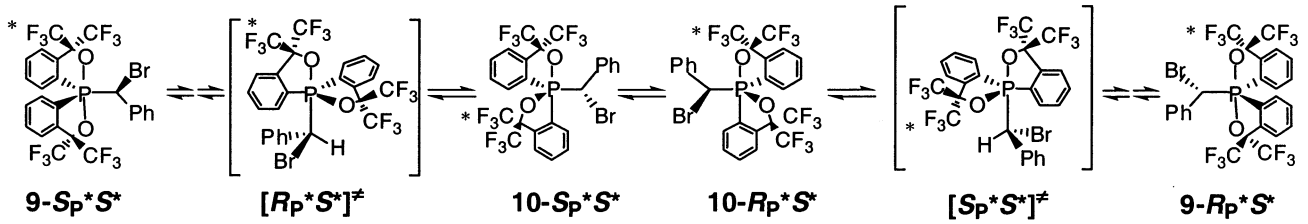

Scheme 10

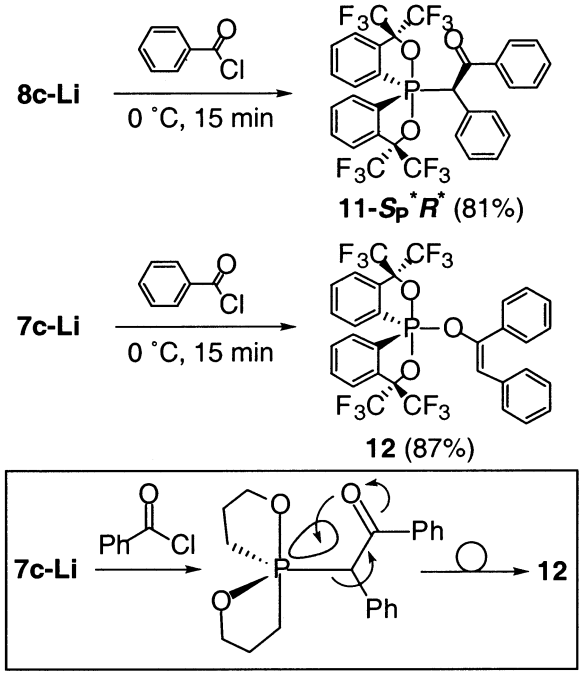

Scheme 11

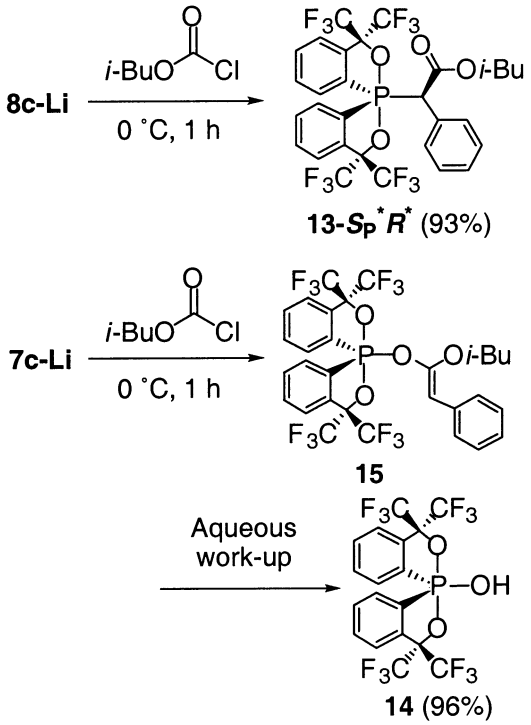

bromination reaction. In the case of the reaction of *O-cis* **1c**, however, the observed ratio is related to the barriers of pseudorotation of the two separate pathways from the initial brominated *O-cis* products to the two diastereomeric products, **9-R_P*S***and **9-S_P*S***. The reason is because (although there could be selectivity in the bromination reaction) this information is lost immediately, since the one-step pseudorotation process involving the monodentate alkyl group as the pivot that inverts the stereochemistry at the phosphorus atom is a low-energy process[12a] and rapid epimerization gives rise to an equilibrium mixture of **10-R_P*S*** and **10-S_P*S*** (Scheme 9). Configurations where a five-membered ring is positioned diequatorially are regarded to be highly unfavorable because of ring strain and thus can be considered as (or structurally very close to) global energy maximums of multistep pseudorotation processes of spirophosphoranes. Therefore, the fact that **9-R_P*S*** was the major isomer for *O-cis* **1c** indicates the preference for [S_P*S*]‡ over [R_P*S*]‡, although the reason is unclear.

Differences in the reactivity of the α-anion between *O-cis* **1c** and *O-trans* **2c** were also observed in acylation. Scheme 10 shows reactions with benzoyl chloride. As reported previously by us, the deprotonation of *O-trans* **2c** with *n*-BuLi, followed by reaction with benzoyl chloride, gave α-benzoylated phosphorane **11-S_P*R*** diastereoselectively.[19] However, the reaction of *O-cis* **1c** under similar conditions provided unexpected phosphorane **12**. Obviously, compound **12** was formed via rearrangement of the benzoylated product followed by pseudorotation. This rearrangement can be rationalized to have been induced by the enhanced electrophilicity of the σ^*_{P-O} orbital. The structure of **12** was confirmed by X-ray analysis (see Supporting Information).

Using isobutyl chloroformate as an electrophile, the reaction proceeded in a similar manner as the reactions in Schemes 8 and 10. *O-trans* **2c** provided only one diastereomer **13-S_P*R***(Scheme 11). On the other hand, the reaction of *O-cis* **1c** gave *O-trans* hydroxyphosphorane **14**. In this case, the reaction product **15** was unstable to water and hydrolyzed during aqueous workup to form **14**. The structure of **13-S_P*R*** was confirmed by X-ray analysis (see Supporting Information).

(ii) Reaction with Aldehydes. Previously, we have reported on the olefin formation reaction of all four diastereomers of *O-trans-β*-hydroxyethylphosphoranes **16**, which were independently prepared (Scheme 12). It was found that olefin formation was stereospecific, that the rate of olefin formation was countercation dependent (K > Na > Li), and that the reaction proceeded at temperatures lower than −40 °C in the case of K^+.[19] Here, the reaction of *O-trans* benzylphosphorane **2c** with PhCHO was first examined.

The reaction smoothly proceeded to afford stilbenes and **14** in high yields (Scheme 13). *Z*-Stilbene was formed predominantly in the reaction, and the *Z*/*E* ratio was up to 80:20 using KH as the base in the presence of 18-crown-6 ether (total yield of stilbene was 98%).

Likewise, we carried out reactions of the corresponding anion of *O-cis* **1c** with PhCHO with KH as the base. To our surprise,

Scheme 12

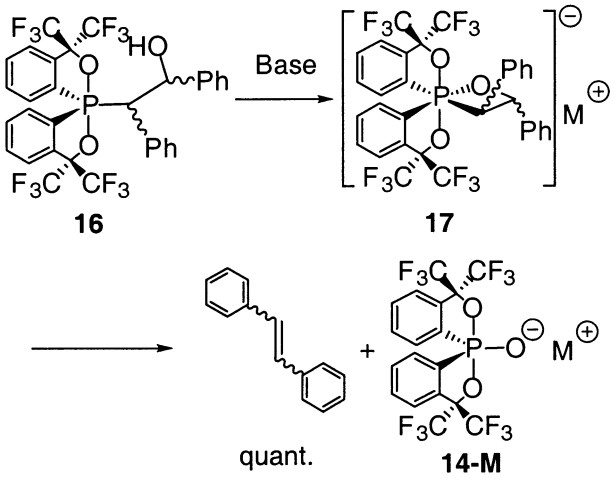

Scheme 13

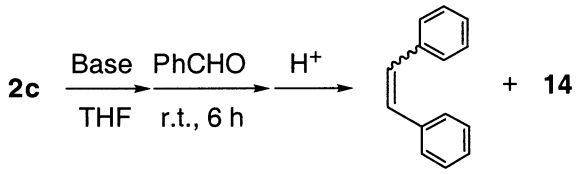

Base	Yield (%)	*Z* : *E*
KH / 18-crown-6	98	80 : 20
n-BuLi	91	59 : 41

Table 3. Total Yield and the Ratio **18A/18B**

base	time (h)	yield (%)	**18A/18B**
n-BuLi	5	43	47:53
	10	42	31:69
	20	45	15:85
KH	5	75	87:13
	10	71	83:17
	20	73	78:22

the adducts **18** (i.e., two diastereomers that are diastereomeric because of the difference in relative configuration upon vicinal carbon atoms) were obtained at ambient temperature, and stilbenes were not formed at all (Scheme 14).

These two diastereomers (**18A** and **B**) could not be separated by TLC. However, after prolonged reaction time (>24 h) using *n*-BuLi as the base, equilibration took place between the *β*-alkoxides of **18A** and **B** to provide only **18B** after aqueous workup of the reaction mixture (Table 3). The structure of **18B** was determined by X-ray analysis to assume the relative configuration of $\boldsymbol{R_P{*}S^{*}S^{*}}$ (Figure 5). Since one-step pseudorotation at the phosphorus atom of *O-cis* spirophosphoranes with

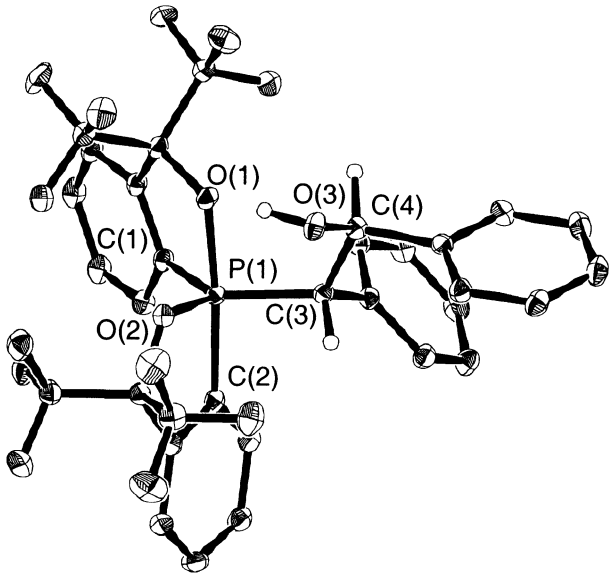

Figure 5. ORTEP drawing of **18B** showing the thermal ellipsoids at the 30% probability level.

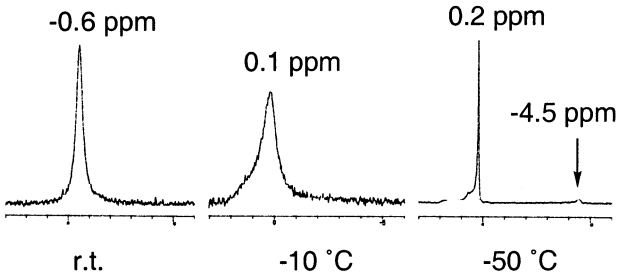

Figure 6. Low-temperature ^{31}P NMR signals for a rapidly equilibrating mixture of **18B**-$\boldsymbol{R_P{*}S^{*}S^{*}}$ and **18B**-$\boldsymbol{S_P{*}S^{*}S^{*}}$.

the monodentate as the pivot is rapid, as described above, **18B** likewise existed as a rapidly equilibrating mixture of $\boldsymbol{R_P{*}S^{*}S^{*}}$ and $\boldsymbol{S_P{*}S^{*}S^{*}}$, each of which could be observed as different ^{31}P NMR signals (δ_P −4.5, 0.2 ppm) at low temperatures in $CDCl_3$ (Figure 6).

Figure 7 shows ^{31}P NMR signals of the reaction of **7c-Li** with PhCHO using *n*-BuLi as the base. The high-field chemical shifts (−100 to ca. −120 ppm) indicate the formation of hexacoordinate phosphorus species, and pentacoordinate species could not be observed. Signals $\mathbf{B_1}$ and $\mathbf{B_2}$ increased with time at the expense of signal **A**, resulting in only signals $\mathbf{B_1}$ and $\mathbf{B_2}$ at the end. Thus, signal **A** corresponds to the hexacoordinate phosphate (**Int-A** in Scheme 16) that affords **18A** by acidic hydrolysis. On the other hand, signals $\mathbf{B_1}$ and $\mathbf{B_2}$ are for the hexacoordinate phosphates (**Int-**$\mathbf{B_1}$ and $\mathbf{B_2}$ in Scheme 16) that lead to **18B** after hydrolysis.

Scheme 14

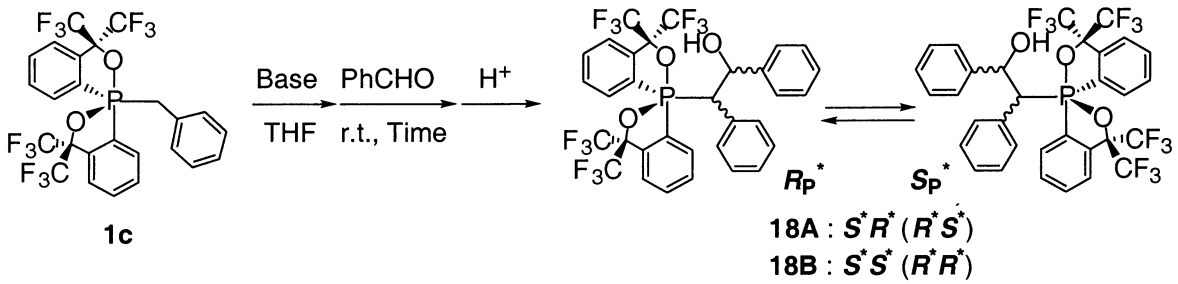

Scheme 15

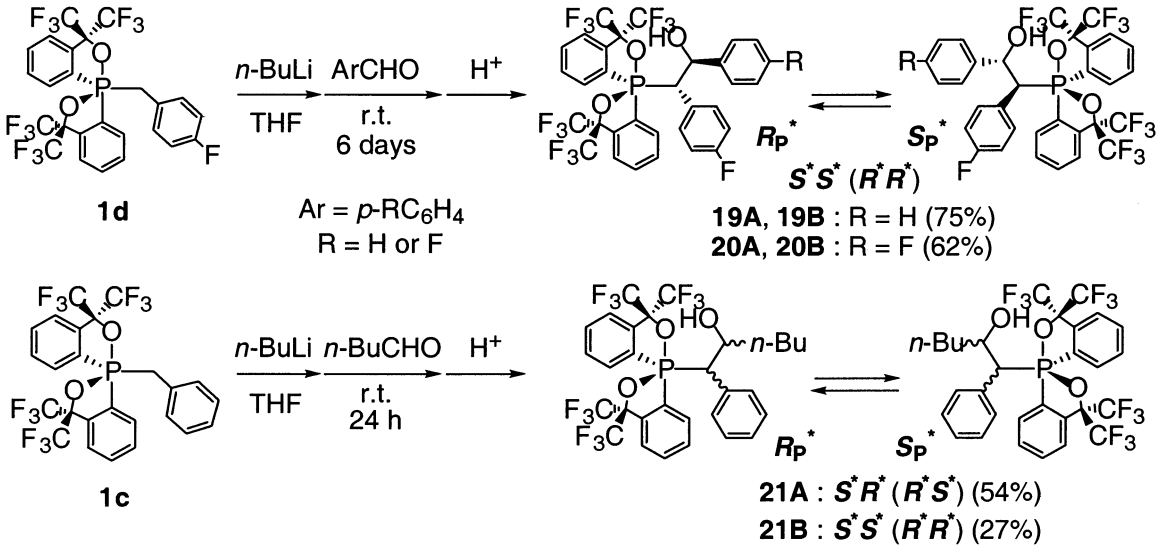

Scheme 16

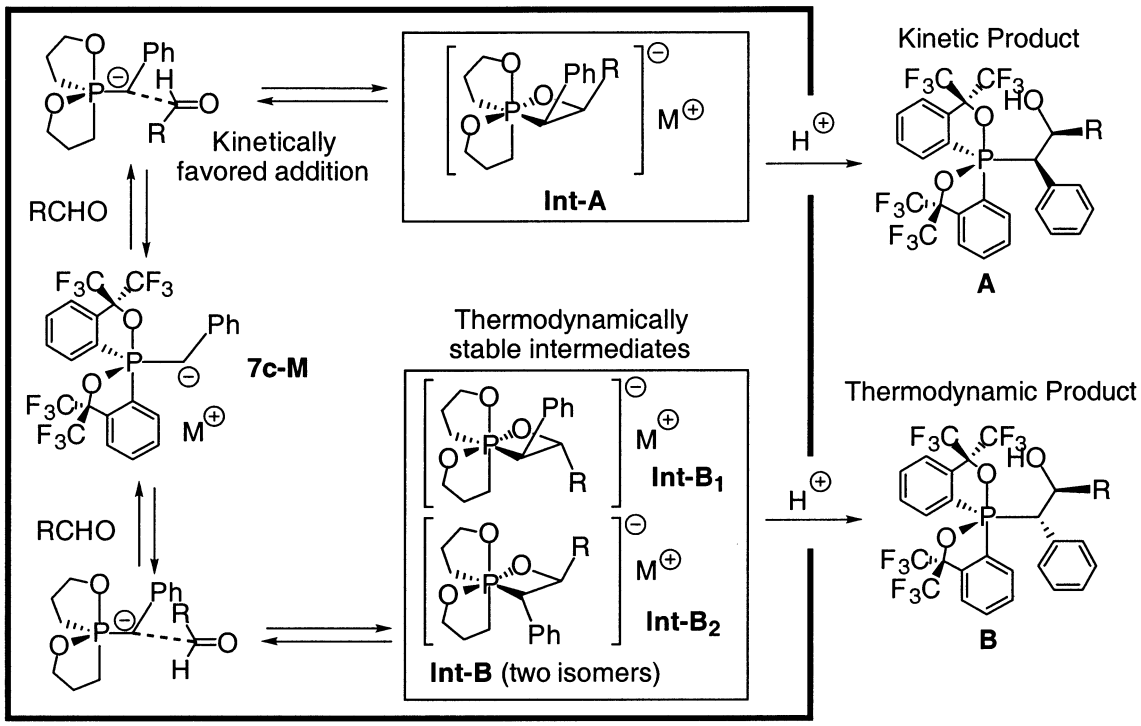

The reaction behavior of the anion from *p*-fluorophenylmethyl derivatives **1d** with PhCHO or (*p*-FC_6H_4)CHO was similar to that of **1c** and PhCHO. The two obtained pairs of diastereomers **19A** and **B** and **20A** and **B** could not be separated in either case. Longer reaction times (6 days; not optimized) were required to obtain single isomers (**19B** and **20B**). These products were characterized by NMR and elemental and X-ray analyses (see Supporting Information) (Scheme 15).

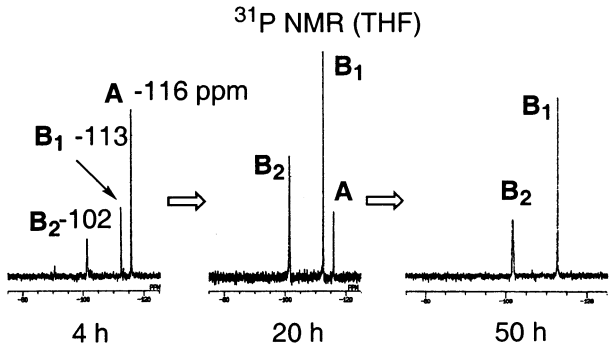

Figure 7. Time course of the ^{31}P NMR signals of the reaction of **7c-Li** with PhCHO.

^{31}P NMR monitoring of the products of the reaction of the anion generated from **1c** with *n*-BuCHO showed slower but similar equilibration. In this case, the diastereomers (**21A** and **B**) could be separated by TLC, and the structure of both **21A** (Figure 8) and **B** (see Supporting Information) could be confirmed by X-ray analysis.

A possible mechanism of the reaction of *O-cis* benzyl anion **7c-M** with RCHO is illustrated in Scheme 16. Kinetically, the addition of RCHO to the anion proceeds in a manner in which the phenyl (the large phosphorus moiety) and the R groups avoid

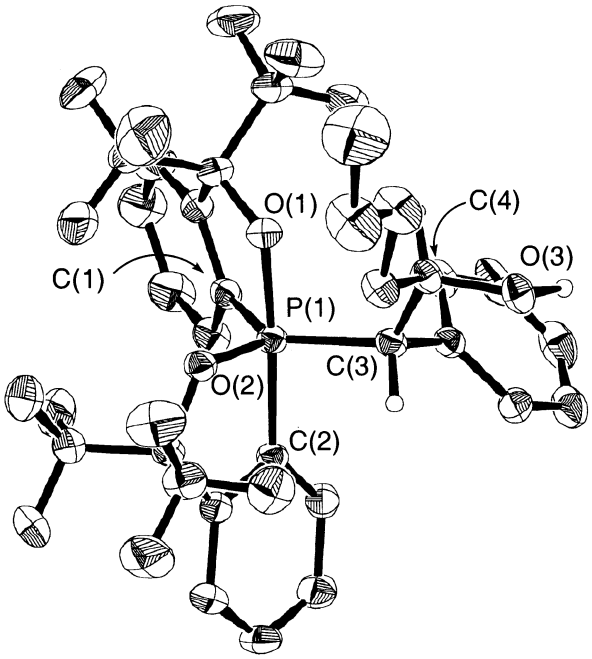

Figure 8. ORTEP drawing of **21A** showing the thermal ellipsoids at the 30% probability level.

mutual steric congestion at the aldol condensation stage, and the resulting phosphate **Int-A**, where the phenyl and the R groups become overlapped by forming the oxaphosphetane ring, is the predominant intermediate. **Int-A** gives isomer **A** by treatment with a proton source. However, **Int-A** is expected to be relatively unstable because of the steric repulsion between the phenyl and the R groups on the four-membered ring, and therefore, retro-aldol cleavage takes place from **Int-A** to regenerate **7c-M**. On the other hand, when the addition proceeds in an opposite manner, intermediates **Int-B** ($\mathbf{B_1} + \mathbf{B_2}$) are generated. Both **Int-B** ($\mathbf{B_1} + \mathbf{B_2}$) isomers are sterically less hindered and should be more stable intermediates than **Int-A**. After equilibrium between **Int-A** and **Int-B** ($\mathbf{B_1} + \mathbf{B_2}$) is established, only **Int-B** ($\mathbf{B_1} + \mathbf{B_2}$) is observed in the reaction solution, and **18B** is obtained as the sole adduct after hydrolysis in this system. **Int-B** ($\mathbf{B_1} + \mathbf{B_2}$) should correspond to the signals $\mathbf{B_1}$ and $\mathbf{B_2}$ in Figure 7. In principle, for the intermediate phosphates, four isomers are conceivable for both **Int-A** and **Int-B**, arising from the fast interconversion upon the phosphorus atom and from the site of ligation of the β-oxide anion (anti to either carbon or oxygen atoms in the equatorial plane). The identities of the intermediate phosphates could not be determined. However, we believe that the observed isomers are the ones in which the β-oxide anion ligates anti to the equatorial oxygen atom, since the formation of the strained four-membered ring should be boosted by the trans influence of the oxygen atom. As for the relative stereochemistry between the phosphorus moiety and the α-substituent, the major product is probably the one having the apical oxygen and the α-substituent in a syn relationship, since interaction between CF_3 (of the inverted Martin ligand) and Ph groups can be avoided. For the phosphate(s) corresponding to signal **A**, the strongly unfavorable doubled interaction in the isomer, which is not shown here, must be the reason only one isomer is observed. The fact that the relative ratio of the **B** ($\mathbf{B_1} + \mathbf{B_2}$) signals was constant throughout the conversion of **Int-A** to **Int-B** coincides with the rapid interconversion upon the phosphorus atom.

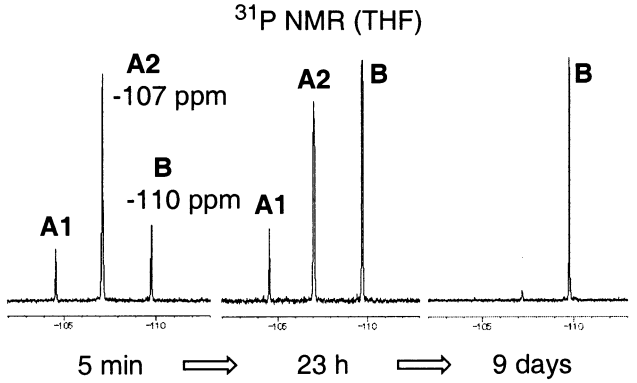

Figure 9. Time course of the ^{31}P NMR signals of the deprotonation reaction of **18B** with KH.

Isolation and Thermolysis of Hexacoordinate Phosphate Bearing an Oxaphosphetane Ring. When the thermodynamic product **18B** was deprotonated by KH in THF to form the hexacoordinate phosphate, three ^{31}P NMR signals (δ_P −104 to ca. −110) were observed in the solution at the initial stage (Figure 9). The ratio of the peaks changed gradually, and finally only a signal at −110 ppm remained after equilibration for 9 days. The fact that only one isomer, which should be sterically the most stable one (**22B-K**), existed in the system indicated the possibility of isolation and stimulated us to investigate the structure. We were successful in obtaining single crystals of the phosphate **22B-K(18-crown-6)** by recrystallizing from a *n*-hexane and CH_2Cl_2 mixture under an inert atmosphere (Scheme 17). Surprisingly, these crystals were stable to air at room temperature for several months. A practical procedure for isolation was as follows: **18B** was deprotonated with KH in CH_2Cl_2 in the presence of 18-crown-6 ether. The remaining KH was removed by filtration, and the resulting solution was allowed to stand for 9 days at room temperature to convert **22A-K(18-crown-6)** to **22B-K(18-crown-6)** completely. Finally, freshly distilled *n*-hexane was carefully added on to the solution, and the resulting two-phase solution was allowed to stand at room temperature to form colorless crystals. The isolated phosphate **22B-K(18-crown-6)** showed a singlet at −113.3 ppm in ^{31}P NMR (CD_3CN), characteristic of a hexacoordinate phosphate. In ^{19}F NMR (CD_3CN), four distinguishable quartets were observed. These observations indicated that **22B-K(18-crown-6)** had a hexacoordinate structure also in polar CD_3CN solution. The X-ray structure of **22B-K(18-crown-6)** is shown in Figure 10. This presents the first structural characterization of a hexacoordinate phosphate bearing an oxaphosphetane ring, which is similar to intermediates in the Wittig reaction involving a pentacoordinate oxaphosphetane. The structure is a slightly distorted octahedral, and the two phenyl groups on the four-membered ring are located trans to each other. The most important finding is that the structure has a configuration that could be assumed to have formed by the attack of the alkoxide anion to the σ^*_{P-O} orbital (anti to the equatorial oxygen atom) of *O-cis* phosphorane **18B**. We[25] and Kawashima et al.[26] have reported recently on the NMR observation of hexacoordinate phosphates (**23**) having an oxaphosphetane ring unsubstituted at the position α to phosphorus. These were prepared from

(25) Kojima, S.; Akiba, K.-y. *Tetrahedron Lett.* **1997**, *38*, 547−550.
(26) Kawashima, T.; Watanabe, K.; Okazaki, R. *Tetrahedron Lett.* **1997**, *38*, 551−554.

Scheme 17

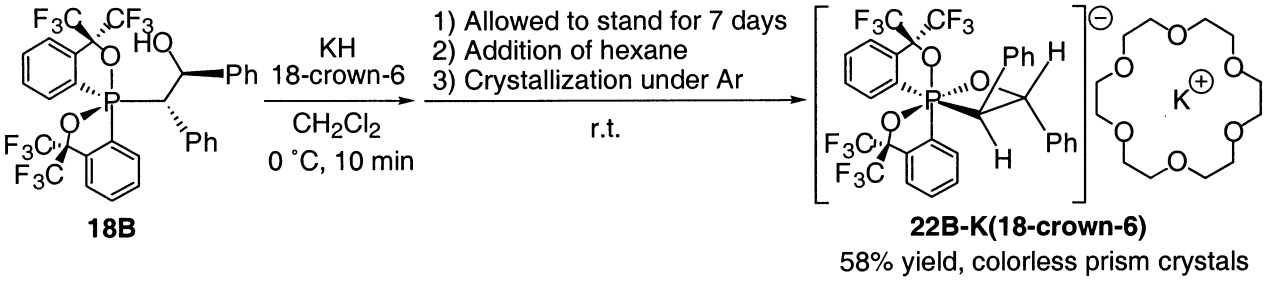

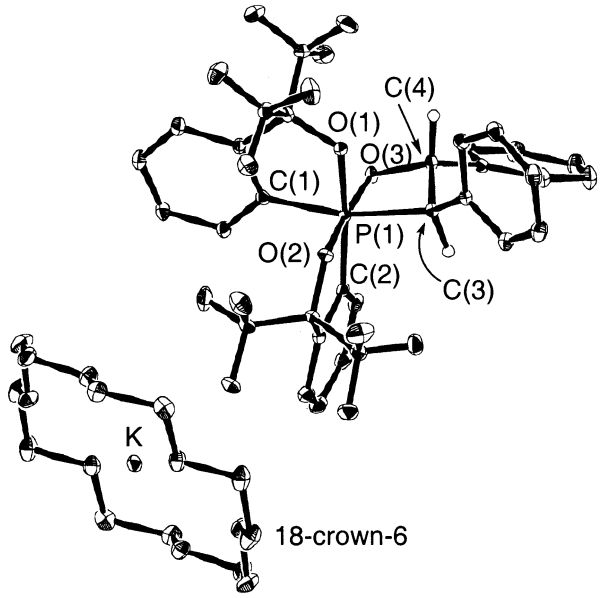

Figure 10. ORTEP drawing of **22B-K(18-crown-6)** showing the thermal ellipsoids at the 30% probability level.

O-trans **24** (Scheme 18). The observations that all hexacoordinate species **23** could be observed at room temperature and were thermally very stable at higher temperatures except **23d** are in contrast with our recent results on hexacoordinate phosphates derived from *O-trans* benzylphosphorane **2c** with PhCHO (Schemes 12 and 13) that were found to be unstable and to easily decompose to give olefin below −40 °C. These differences should be due to the relatively low energy for the cleavage of the P−C(benzyl) bond in **17** (in Scheme 12), showing that substituents are important factors in determining the stability of oxaphosphetanes. Compound **23d**, having strongly electronegative groups (CF_3), gave olefin after heating to 80−100 °C, indicating that the P−Cα bond energy is important. On the basis of these facts, it is quite noteworthy that **22A** and **B** having a P−C(benzyl) bond are so stable, clearly showing that the trans influence of the P−O bond serves to stabilize the anionic species as a whole and even the otherwise weak P−C(benzyl) bond, by the inductive electron-withdrawing nature of the oxygen atom. The thermolysis of **22** will be discussed later (vide infra).

Since single crystals of **23** could not be obtained, the structures of **23** were estimated based on NMR. We cannot confirm the previous structural discussions with certainty because of the difference in substituents between **22** and **23**. However, **isomer 3** (in Scheme 18), which was proposed by Kawashima to be one of the three isomers,[26] seems to be incorrect because **isomer 3** is expected to give an *O-cis* pentacoordinate adduct after treatment with water just like with **22**. In our experimental results, not any formation of *O-cis* pentacoordinate compounds was indicated after aqueous treatment of **23**.[25]

A possible interpretation of the observations is illustrated in Scheme 19. Compound **18B** exists as the equilibrium mixture of $\boldsymbol{R_P{*}S^{*}S^{*}}$ and $\boldsymbol{S_P{*}S^{*}S^{*}}$, as previously shown in Scheme 14. The X-ray structure of **18B** reveals that the configuration preferred in the solid state corresponds to $\boldsymbol{R_P{*}S^{*}S}$, and hydrogen bonding is observed between the hydroxy hydrogen atom and the apical oxygen atom. Because of this hydrogen bonding, steric repulsion between the phenyl group α to phosphorus and the CF_3 group of the inverted Martin ligand can be envisioned in the $\boldsymbol{S_P{*}S^{*}S}$ isomer. Thus, it seems reasonable to assume that the equilibrium lies to the side of $\boldsymbol{R_P{*}S^{*}S^{*}}$ also in solution. If the ratio of the equilibrium $\boldsymbol{R_P{*}S^{*}S^{*}}$/ $\boldsymbol{S_P{*}S^{*}S^{*}}$ is maintained after deprotonation to some degree and the resulting alkoxide anions cyclize rapidly, phosphate **22A-K** would be the initial major product as observed as signal **A2** (or **A1**) in NMR (Figure 9). However, phosphate **22A-K** is unstable because of steric repulsion between the phenyl and the trifluoromethyl groups; therefore, ring cleavage reaction of the P−O bond of the oxaphosphetane ring in **22A-K** takes place. On the other hand, phosphate **22B-K** generated from the minor alkoxide $\boldsymbol{S_P{*}S^{*}S^{*}}$ has a less hindered structure and therefore should be the most stable isomer. On the basis of these considerations, signal **B** in Figure 9 corresponds to the phosphate **22B-K** in Scheme 19, and one of signals **A1** and **A2** should correspond to **22A-K**. Since the reaction time for the equilibration from **22A-K** to **22B-K** was quite long and not well-reproducible, trace amounts of water probably coordinate to the oxygen of the four-membered ring and accelerate the conversion. The identity of the species corresponding to signal **A1** (or **A2**) eludes us. One possibility is that it is a species formed by the oxide attack anti to the equatorial carbon atom. As experimentally demonstrated (vide supra), this would be an unfavorable process. However, because of the constraint imposed by the tether, some other factors such as sterics might be able to facilitate an intramolecular nucleophilic attack of the oxide to the equatorial carbon.

Selected structural parameters for **18B** and **22B-K(18-crown-6)** are summarized in Table 4. Upon conversion of **18B** to **22B-K(18-crown-6)**, the equatorial bond distances P(1)−O(2), P(1)−C(1), and P(1)−C(3) increased remarkably. These increments were due to the transformation of the equatorial (sp^2) bonds of **18B** to the weaker hypervalent (3c−4e) bonds of **22B-K(18-crown-6)**. Especially, the increment of P(1)−O(2) was 0.135 Å (+8.2%). This indicates the large flexibility of the P−O bond as compared with the P−C bonds (+3.0%) of P(1)−C(1) and P(1)−C(3). It could be that this nature prevents the P(1)−C(3)

Scheme 18

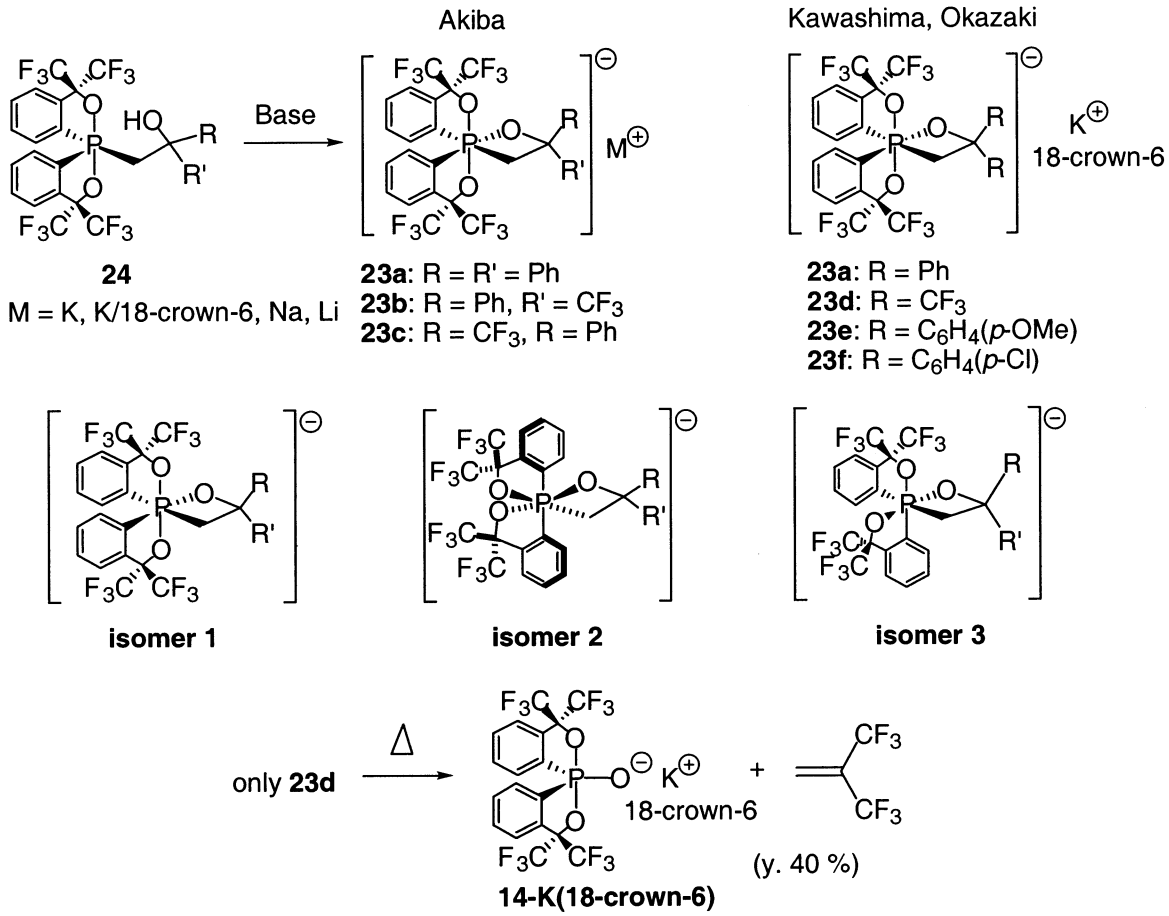

Scheme 19

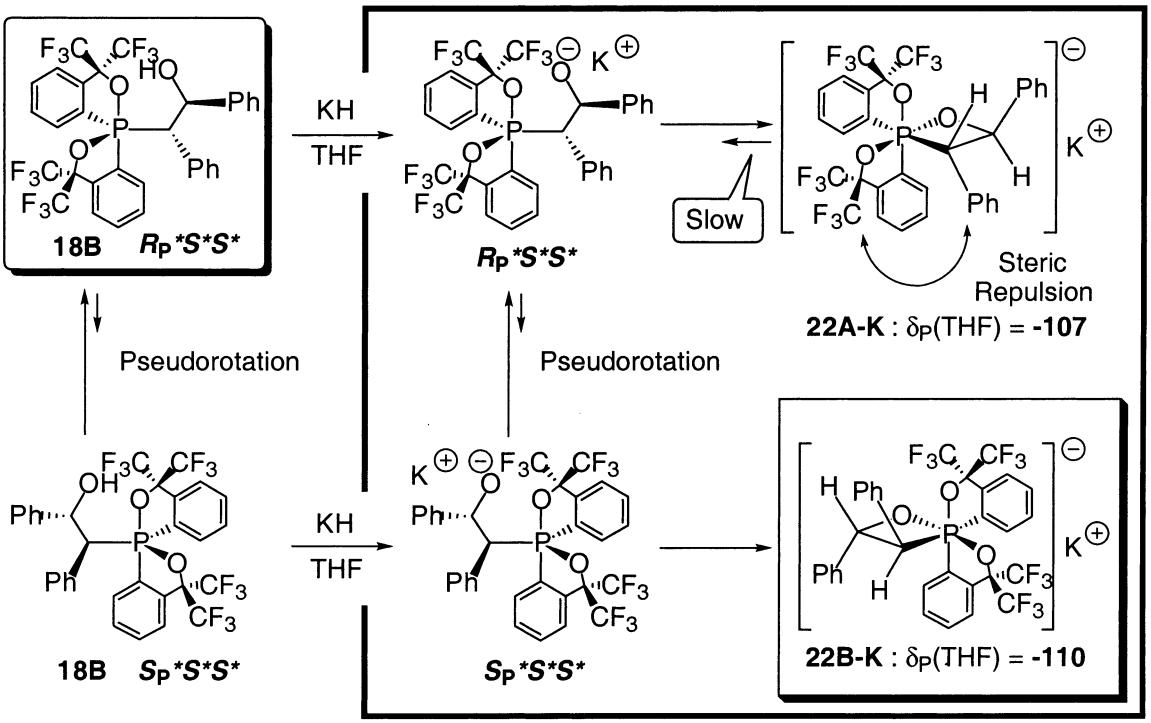

bond from being weakened enough to cleave and furnish olefins upon the increase of the coordination number from 5 to 6. It is noteworthy here that there is almost no change of bond lengths of the original hypervalent bonds of P(1)−O(1) and P(1)−C(2).

A structural comparison of the oxaphosphetane moiety between **22B-K(18-crown-6)** and pentacoordinate oxaphosphetanes **25**,[27] **26**,[28] **27**,[29] and **28**[29] was carried out (Figure 11 and Table 5). Compounds **25** and **26** were isolated by Kawashima-

Table 4. Comparison of Bond Distances (Å) between **18B** and **22B-K(18-crown-6)**

	18B	22B-K(18-crown-6)	increment (Å)	
P(1)−O(1)	1.793(1)	1.782(1)	−0.011(2)	(−0.6%)
P(1)−O(2)	1.653(1)	1.788(1)	+0.135(2)	(+8.2%)
P(1)−O(3)		1.731(1)		
P(1)−C(1)	1.835(2)	1.891(2)	+0.056(4)	(+3.1%)
P(1)−C(2)	1.872(2)	1.872(2)	±0.000(4)	(±0.0%)
P(1)−C(3)	1.869(2)	1.926(2)	+0.057(4)	(+3.0%)
O(3)−C(4)	1.425(2)	1.439(2)	+0.014(4)	(+1.0%)
C(3)−C(4)	1.558(2)	1.533(2)	−0.025(4)	(−1.6%)

Table 5. Selected Structural Parameters for the Oxaphosphetane Moiety

	P−O (Å)	P−Cα (Å)	O−P−Cα (deg)
22B-K(18-crown-6)	1.731(1)	1.926(2)	75.97(6)
25[27]	1.728(2)	1.808(4)	77.4(1)
26[28]	1.781(6)	1.823(9)	75.5(3)
27[29]	1.748(3)	1.823(4)	77.2(1)
28[29]	1.657(3)	1.916(5)	76.7(2)

Okazaki's group, and compounds **27** and **28** were isolated in our laboratory. It should be noted that compound **28** has the oxygen in the oxaphosphetane ring at the equatorial position, and therefore **28** is an *O-cis* phosphorane. The most significant difference in **22B-K(18-crown-6)** as compared with **25**−**27** is the P−Cα bond distance. That of the former is 1.926(2) Å and is much longer than those of the latter three, which are ca. 1.82 Å (Table 5). This result reflects the differences of the bonding nature (i.e., P−Cα in **22B-K(18-crown-6)** is a weak hypervalent (3c−4e) bond, while those of **25**−**27** are essentially sp^2 bonds). On the other hand, the length of P−Cα in **28** is comparable with that of **22B-K(18-crown-6)**. This observation is quite reasonable, taking into account the fact that this bond in **28** is also a hypervalent bond (apical bond).

Finally, we investigated the thermal decomposition of **22B-K(18-crown-6)** in solution. **22B-K(18-crown-6)** was heated at 60 °C in THF for 4 days to afford *trans*-stilbene, quantitatively (Scheme 20). Kinetic measurements for the reaction were carried out by NMR to determine activation parameters using the Eyring plot (Figure 12). This is in great contrast to the decomposition of 12-P-6 phosphates with K^+ as the countercation generated from isomeric *O-trans* phosphoranes (Scheme 21), which occurred at temperatures even below −40 °C.[19] A countercation effect similar to that observed for *O-trans* phosphoranes was observed when the decomposition rate of **22B-K** was compared with that of **22B-K(18-crown-6)** at 80 °C (Figure 13). The decomposition of the latter was 37 times faster than that of the former. Since crown ether was not used in the decomposition of *O-trans* phosphoranes (Na^+ salt), the actual difference in the decomposition rate between the phosphate from *O-cis* phosphorane and that from the *O-trans* isomer would be even larger. On the basis of these results, **22B-K(18-crown-6)** was revealed to be thermodynamically quite stable, although the phosphate was a hexacoordinate compound with elongated weakened bonds.

Kinetic parameters of the decomposition of **22B-K(18-crown-6)** were obtained as $\Delta H^{\ddagger} = 27.1 \pm 0.8$ kcal/mol, $\Delta S^{\ddagger} = 0.4 \pm 2.5$ eu, and $\Delta G^{\ddagger}_{298} = 27.0$ kcal/mol. The activation entropy ($\Delta S^{\ddagger}$) for the decomposition was close to zero. In this case, the P−C bond of the oxaphosphetane ring that is to be cleaved is already elongated and weakened as a 3c−4e bond; thus, structural change may not be essential for the decomposition of **22B-K(18-crown-6)**. On the other hand, the activation entropies of the decompositions for **25** ($\Delta S^{\ddagger} = -4.1 \pm 1.2$ eu)[27] and **26** ($\Delta S^{\ddagger} = -8.8 \pm 1.2$ eu)[28] were reported as negative values. In these cases, the negative values can be considered to be due to considerable change of the structure of the oxaphosphetane ring before the formation of olefinic products.

In summary, we have recently discovered a method of preparing a novel group of anti-apicophilic spirophosphoranes (*O-cis*), in which the usually more apicophilic oxygen atom and the less apicophilic carbon atom have exchanged places as thermodynamically less stable isomers of phosphoranes of

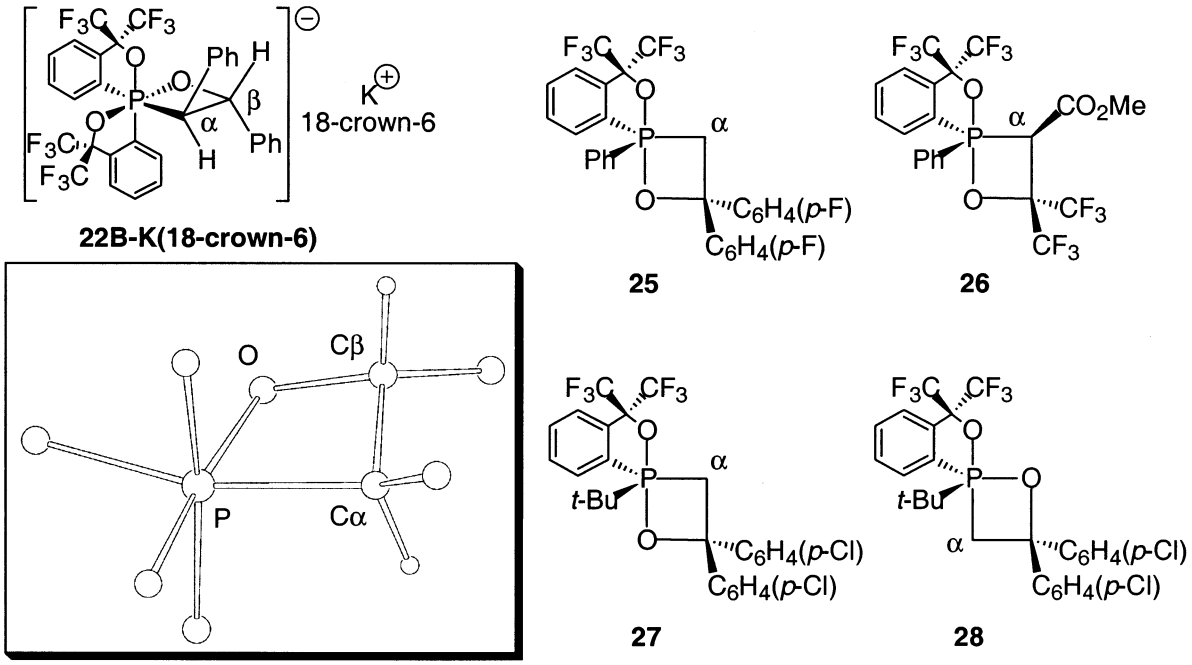

Figure 11. Reported oxaphosphetanes and the structure of the oxaphosphetane moiety of **22B-K(18-crown-6)**.

Scheme 20

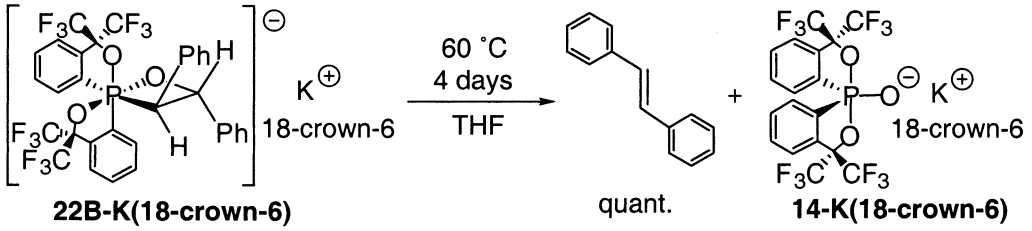

22B-K(18-crown-6) 14-K(18-crown-6)

Scheme 21

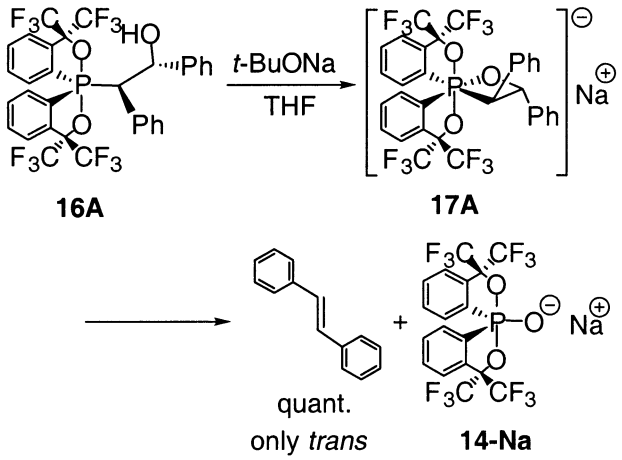

16A 17A 14-Na

$\Delta H^{\neq}$ = 12.6 ± 0.8 kcal/mol

$\Delta S^{\neq}$ = -23.0 ± 3.2 e.u.

$\Delta G^{\neq}_{298}$ = 19.5 kcal/mol

ordinary *O-trans* configuration. This has paved the way for the first examination of the difference in reactivity between phosphoranes differing in configuration only about the phosphorus atom. A structural divergence between the two isomers that catches the eye is the presence of a P−O bond in the equatorial plane in *O-cis* phosphoranes. This is expected to provide a rather low-lying σ_{P-O}* orbital capable of accepting electron density, whereas the corresponding bond in *O-trans* phosphoranes is a P−C bond that should be less capable of accepting electrons. The equatorial P−O delocalization effect was demonstrated here in two kinds of phenomena. One is in the reaction toward the phosphorus atom, and the other is in the acidity of the carbon α to the phosphorus atom. For the former, enhanced reactivity in nucleophilic reactions toward the phosphorus atom was observed in the reaction of **1** (*O-cis*) with fluoride, alkyllithium, and rearrangement of the carbonyl oxygen of the phenacyl group compared with **2** (*O-trans*). Another related observation was the great stabilization of newly formed hypervalent bonds in hexacoordinate phosphates formed by intramolecular attack of the oxide anion anti to the equatorial oxygen in **1** (*O-cis*), whereas corresponding phosphates generated from **2** (*O-trans*) have been found to decompose much more easily. For the latter, the difference in the stability of carbanions α to the phosphorus in **1** and **2** has clearly been demonstrated. Theoretical calculations on **1**, **2** and their conjugated bases **7**, **8** supported these

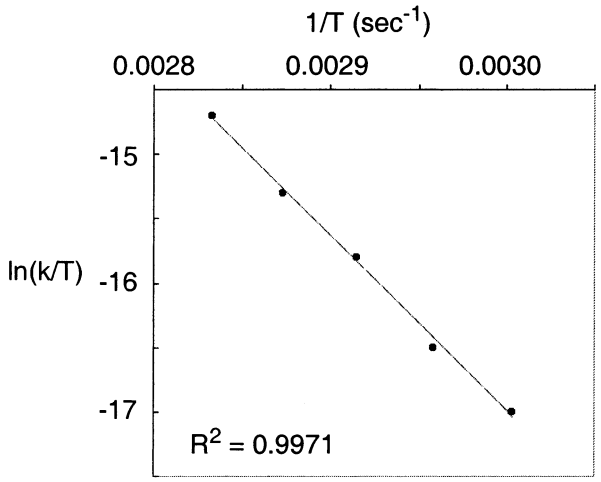

$\Delta H^{\neq}$ = 27.1 ± 0.8 kcal/mol

$\Delta S^{\neq}$ = 0.4 ± 2.5 e.u.

$\Delta G^{\neq}_{298}$ = 27.0 kcal/mol

Figure 12. Eyring plot of the rate constants for the thermal decomposition of **22B-K(18-crown-6)**.

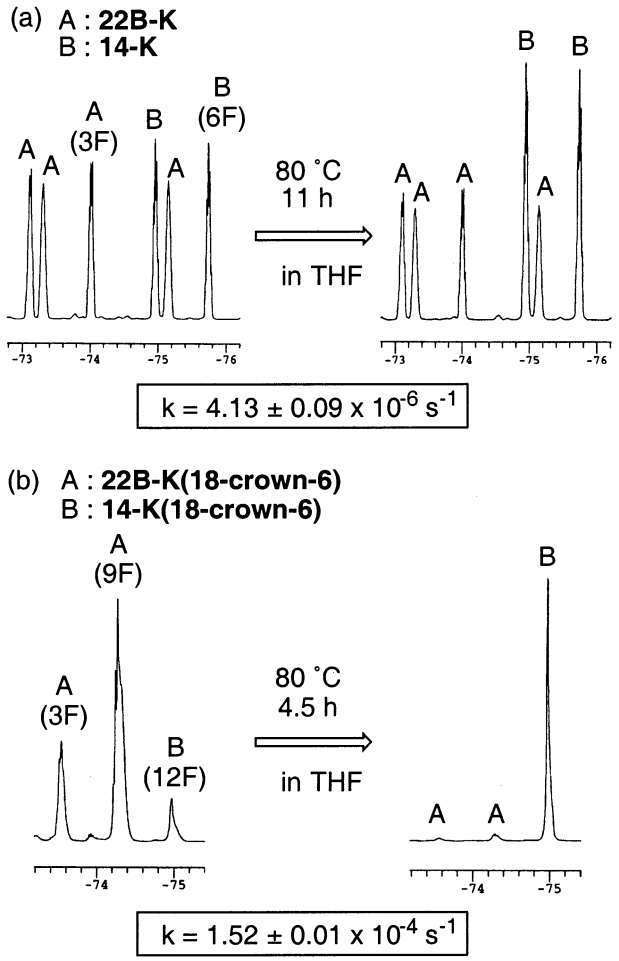

Figure 13. Comparison of the rates of the thermal decomposition of **22B-K** and **22B-K(18-crown-6)**.

experimental results and gave clearer insights into the present chemistry. The results presented here show that anti-apicophilic phosphoranes have provided new insights into a full picture of the nature of the pentacoordinate state of phosphorus. Here, we have presented a new, unique, and well-designed example in the chemistry of stereoelectronic effects. Further investigations concerning this unique group of compounds are currently ongoing.

Experimental Section

General. Melting points were measured with a Yanaco micro melting point apparatus and are uncorrected. ^{1}H NMR (400 MHz), ^{13}C NMR (100 MHz), ^{19}F NMR (376 MHz), and ^{31}P NMR (162 MHz) spectra were recorded on a JEOL EX-400 spectrometer. ^{1}H NMR chemical shifts (δ) are given in ppm downfield from Me_4Si, determined by residual chloroform ($\delta = 7.26$). ^{13}C NMR chemical shifts (δ) are given in ppm downfield from Me_4Si, determined by chloroform-*d* ($\delta = 77.0$). ^{19}F NMR chemical shifts (δ) are given in ppm downfield from external $CFCl_3$. ^{31}P NMR chemical shifts (δ) are given in ppm downfield from external 85% H_3PO_4. Elemental analyses were performed on a Perkin-Elmer 2400 CHN elemental analyzer.

All reactions were carried out under N_2 or Ar. THF and Et_2O were freshly distilled from Na-benzophenone, *n*-hexane was distilled from Na, and all other solvents were distilled from CaH_2. Preparative thin-layer chromatography was carried out on plates of Merck silica gel 60 GF_{254}. Merck silica gel 60 was used for column chromatography.

[*TBPY*-5-12]-1-Phenylmethyl-3,3,3′,3′-tetrakis(trifluoromethyl)-1,1′-spirobi[3*H*,2,1,λ^5-benzoxaphosphole] (1c). *n*-BuLi (1.50 M hexane solution, 19.3 mL, 30.3 mmol) was added to a mixture of *t*-BuOK (3.41 g, 30.4 mmol) and toluene (3.30 mL, 31.0 mmol) suspended with *n*-hexane (15 mL) at room temperature. This mixture was vigorously stirred for 1 h. At 0 °C, Et_2O (35 mL) was added to the mixture, and then a solution of **3** (5.10 g, 9.88 mmol) in Et_2O (60 mL) was transferred dropwise. The mixture was stirred for 9 h at room temperature. Iodine (7.90 g, 31.1 mmol) was added at −78 °C, and the resulting mixture was stirred for 1 h. After the cooling bath was removed, stirring was continued until the color of the mixture became dark-brown. After the solution was treated with $Na_2S_2O_3$ (aq) (100 mL), the mixture was extracted with Et_2O (100 mL × 2), and the ethereal layer was washed with brine (100 mL) and dried over anhydrous $MgSO_4$. The crude product was subjected to column chromatography (*n*-hexane/CH_2Cl_2 = 2:1). The resulting pale red solid was washed with *n*-hexane to yield a crystalline white solid of **1c** (4.73 g, 7.81 mmol, 79.0%). Colorless crystals suitable for X-ray analysis were obtained by recrystallization from CH_3CN. ^{1}H NMR ($CDCl_3$, δ) 7.73−7.71 (m, 2H), 7.66−7.61 (m, 2H), 7.58−7.51 (m, 4H), 7.14−7.11 (m, 3H), 6.98−6.97 (m, 2H), 3.96 (d, 2H, $^2J_{P-H} = 10.7$ Hz); ^{13}C NMR ($CDCl_3$, δ) 134.5 (d, $^2J_{C-P} = 16.7$ Hz), 134.4 (d, $^1J_{C-P} = 82.5$ Hz), 132.4 (d, $J_{C-P} = 12.5$ Hz), 132.2 (d, $J_{C-P} = 2.5$ Hz), 131.3 (d, $J_{C-P} = 10.8$ Hz), 130.5 (d, $J_{C-P} = 7.5$ Hz), 129.8 (d, $J_{C-P} = 10.0$ Hz), 128.2 (d, $J_{C-P} = 4.2$ Hz), 126.8 (d, $J_{C-P} = 5.0$ Hz), 125.4 (d, $J_{C-P} = 10.0$ Hz), 122.1 (dq, $J = 8.3$ Hz, $^1J_{C-F} = 286$ Hz), 121.8 (q, $^1J_{C-F} = 287$ Hz), 79.8 (septet, $^2J_{C-F} = 31.7$ Hz), 47.6 (d, $^1J_{C-P} = 109$ Hz); ^{19}F NMR ($CDCl_3$, δ) −75.1 (q, 6F, $^4J_{F-F} = 8.6$ Hz), −76.3 (q, 6F, $^4J_{F-F} = 8.6$ Hz); ^{31}P NMR ($CDCl_3$, δ) −8.0; mp 134−135 °C (decomp). Anal. Calcd for $C_{25}H_{15}F_{12}O_2P$: C, 49.52; H, 2.49. Found: C, 49.77; H, 2.39.

[*TBPY*-5-11]-1-Phenylmethyl-3,3,3′,3′-tetrakis(trifluoromethyl)-1,1′-spirobi[3*H*,2,1,λ^5-benzoxaphosphole] (2c).[19] To a Et_2O (50 mL) solution of **3** (4.07 g, 7.88 mmol) was added DBU (1.80 mL, 12.0 mmol) at room temperature. After the mixture was stirred for 30 min, benzyl bromide (1.50 mL, 12.6 mmol) was added. The mixture was stirred for 7 h at room temperature. After the solution was treated with water (100 mL), the mixture was extracted with Et_2O (100 mL × 2), the ethereal layer was washed with brine (100 mL), and the extract was dried over $MgSO_4$. The crude white solid was recrystallized from *n*-hexane/CH_2Cl_2 to afford colorless crystals of **2c** (4.34 g, 7.15 mmol, 90.7%). ^{1}H NMR ($CDCl_3$, δ) 8.24 (dd, 2H, $J = 10.7$, 8.1 Hz), 7.71−7.57 (m, 6H), 7.15−7.08 (m, 3H), 6.99−6.96 (m, 2H), 3.76 (dd, 1H, $^2J_{P-H} = 15.6$ Hz, $^2J_{H-H} = 13.7$ Hz), 3.71 (dd, 1H, $^2J_{P-H} = 13.7$ Hz, $^2J_{H-H} = 13.7$ Hz); ^{19}F NMR ($CDCl_3$, δ) −74.6 (q, 6F, $^4J_{F-F} = 9.8$ Hz), −75.0 (q, 6F, $^4J_{F-F} = 9.8$ Hz); ^{31}P NMR ($CDCl_3$, δ) −22.0; mp 128−129 °C. Anal. Calcd for $C_{25}H_{15}F_{12}O_2P$: C, 49.52; H, 2.49. Found: C, 49.25; H, 2.18.

Observation of 12-P-6 Phosphate Bearing a P−F Bond (4). To a THF (0.6 mL) solution of **1b** (25 mg, 0.044 mmol) in an NMR tube was added TBAF (tetra-*n*-butylammonium fluoride, 1.0 M solution in THF, 0.05 mL, 0.05 mmol) at room temperature. Then the NMR tube was loaded into an NMR spectrometer (JEOL EX-400) at −30 °C. After 10 min, ^{31}P and ^{19}F NMR spectra were recorded. ^{19}F NMR (THF, δ) −51.4 (**4**, br d, 1F, $^1J_{P-F} = 706$ Hz), −72.8 (**1b**, br s, 6F), −73.2 (**4**, br s, 3F), −74.1 (**4**, br s, 9F), −75.3 (**1b**, br s, 6F); ^{31}P NMR (THF, δ) −0.8 (**1b**, s), −105.0 (**4**, d, $^1J_{P-F} = 706$ Hz); **1b**/**4** = ca. 1:1.

Reaction of the α-Anion of 2c (8a-K(18-crown-6)) with PhCHO. A THF (1.5 mL) solution of **2c** (182 mg, 0.301 mmol) and 18-crown-6 ether (83.0 mg, 0.314 mmol) was added to a THF (0.5 mL) suspension of KH (excess), and then the mixture was stirred for 20 min at room temperature. After removal of KH by filtration and washing with THF (1 mL), benzaldehyde (0.04 mL, 0.39 mmol) was added at 0 °C. The mixture was stirred for 6 h at room temperature, and then the reaction was quenched with aqueous NH_4Cl. The mixture was extracted with Et_2O (80 mL), and the combined organic solution was washed with brine (50 mL) and dried over anhydrous $MgSO_4$. After the solvents were removed by evaporation, the crude product was subjected to TLC (*n*-hexane) to afford *cis*-stilbene (42.1 mg, 0.234 mmol, 77.6%) and *trans*-stilbene (10.8 mg, 0.060 mmol, 19.9%). Total yield of stilbene was 97.5% (cis/trans = 80:20). *cis*-Stilbene ^{1}H NMR ($CDCl_3$, δ): 7.29−7.20 (m, 10H), 6.62 (s, 2H). *trans*-Stilbene ^{1}H NMR ($CDCl_3$, δ): 7.55 (d, 4H, $J = 7.2$ Hz), 7.39 (t, 4H, $J = 7.2$ Hz), 7.29 (t, 2H, $J = 7.2$ Hz), 7.14 (s, 2H).

Synthesis of 18B. To a THF (15 mL) solution of **1c** (912 mg, 1.50 mmol) was added *n*-BuLi (1.50 M hexane solution, 1.10 mL, 1.65 mmol) at 0 °C. The mixture was stirred for 20 min at 0 °C, and then benzaldehyde (0.18 mL, 1.77 mmol) was added. The mixture was stirred for 64 h at room temperature, and then the reaction was quenched with aqueous NH_4Cl. The mixture was extracted with Et_2O (150 mL), and the extract was washed with brine (150 mL) and dried over anhydrous $MgSO_4$. After the solvents were removed by evaporation, the crude product was separated by TLC (*n*-hexane/benzene = 1:5) to afford a white solid of **18B** (620 mg, 0.870 mmol, 57.8%). Colorless crystals suitable for X-ray analysis were obtained by recrystallization from $CDCl_3$. ^{1}H NMR ($CDCl_3$, δ) 7.86−7.84 (m, 1H), 7.71−7.68 (m, 2H), 7.61−7.46 (m, 3H), 7.31−7.27 (m, 1H), 7.13−6.88 (m, 8H), 6.54 (br, 3H), 5.20−5.15 (m, 1H), 4.50−4.00 (br, 1H), 3.72−3.69 (m, 1H); ^{19}F NMR ($CDCl_3$, δ) −74.3 (br s, 3F), −74.6 (br s, 3F), −75.2 (br s, 3F), −76.0 (br s, 3F); ^{31}P NMR ($CDCl_3$, δ) −0.6 (br); mp 148−149 °C (decomp). Anal. Calcd for $C_{32}H_{21}F_{12}O_3P$: C, 53.94; H, 2.97. Found: C, 53.99; H, 3.08.

Isolation of 12-P-6 Phosphate Bearing an Oxaphosphetane Ring (22B-K(18-crown-6)). 18B (299 mg, 0.420 mmol) and 18-crown-6 ether (113 mg, 0.428 mmol) were dissolved into CH_2Cl_2 (4 mL), and then the solution was added to a CH_2Cl_2 (1 mL) suspension of KH (excess) at 0 °C. The mixture was stirred for 10 min, and then the remaining KH was removed by filtration and washed with CH_2Cl_2 (1 mL). The Schlenk apparatus was sealed, and the resulting pale yellow filtrate was allowed to stand for 7 days. Dry *n*-hexane was slowly added so as to create a two-phase solution, which was allowed to stand for 6

(27) Kawashima, T.; Kato, K.; Okazaki, R. *J. Am. Chem. Soc.* **1992**, *114*, 4008−4010. Correction: *J. Am. Chem. Soc.* **1998**, *120*, 6848.
(28) Kawashima, T.; Kato, K.; Okazaki, R. *Angew. Chem., Int. Ed. Engl.* **1993**, *32*, 869−870. Correction: *Angew. Chem., Int. Ed. Engl.* **1998**, *37*, 1606.
(29) Kojima, S.; Sugino, M.; Matsukawa, S.; Nakamoto, M.; Akiba, K.-y. *J. Am. Chem. Soc.* **2002**, *124*, 7674−7675.

days at room temperature under a flow of N_2. The resulting colorless crystals of **22B-K(18-crown-6)** were collected, washed with dry *n*-hexane (10 mL) and dry Et_2O (5 mL), and dried in vacuo. Yield: 249 mg, 0.245 mmol, 58.4%. The crystals were stored under N_2. ^{1}H NMR (CD_3CN, δ) 8.16 (t, 1H, $J_{H-H} = 6.7$ Hz), 7.64 (m, 2H), 7.49 (d, 1H, $J_{H-H} = 6.7$ Hz), 7.45−7.37 (m, 3H), 7.24−7.11 (m, 8H), 7.05−7.02 (m, 1H), 6.91 (dd, $^3J_{P-H} = 12.5$ Hz, $^3J_{H-H} = 7.3$ Hz), 5.89 (dd, $^3J_{P-H} = 11.9$ Hz, $^3J_{H-H} = 7.6$ Hz), 5.28 (dd, $^2J_{P-H} = 2.7$ Hz, $^3J_{H-H} = 9.4$ Hz), 3.80 (dd, $^3J_{P-H} = 12.8$ Hz, $^3J_{H-H} = 9.4$ Hz), 3.55 (s, 24H); ^{19}F NMR (CD_3CN, δ) −74.6 (br s, 3F), −74.7 (m, 6F), −74.9 (br s, 3F); ^{31}P NMR (CD_3CN, δ) −113.3; mp >165 °C (decomp). Anal. Calcd for $C_{44}H_{44}F_{12}KO_9P$: C, 52.07 H, 4.37. Found: C, 51.95; H, 4.24.

Acknowledgment. The authors are grateful to Central Glass Co. Ltd. for a generous gift of hexafluorocumyl alcohol. Partial support of this work through Grant-in-Aid for Scientific Research (Nos. 09239103, 09440218, 11166248, 11304044, 12304044) provided by the Ministry of Education, Culture, Science, Sports, and Technology of the Japanese Government is heartily acknowledged.

Supporting Information Available: Experimental procedures, details of the kinetic measurements, and details for X-ray analysis. This material is available free of charge via the Internet at http://pubs.acs.org.

JA026776C